Chapter 3

Isotropic anelastic media

When the velocity of transmission of a wave in the second medium, is greater than that in the first, we may, by sufficiently increasing the angle of incidence in the first medium, cause the refracted wave in the second to disappear [critical angle]. *In this case, the change in the intensity of the reflected wave is here shown to be such that, at the moment the refracted wave disappears, the intensity of the reflected* [wave] *becomes exactly equal to that of the incident wave. If we moreover suppose the vibrations of the incident wave to follow a law similar to that of the cycloidal pendulum, as is usual in the Theory of Light, it is proved that on farther increasing the angle of incidence, the intensity of the reflected wave remains unaltered whilst the phase of the vibration gradually changes. The laws of the change of intensity, and of the subsequent alteration of phase, are here given for all media, elastic or non-elastic. When, however, both the media are elastic, it is remarkable that these laws are precisely the same as those for light polarized in a plane perpendicular to the plane of incidence.*

George Green (Green, 1838)

The properties of viscoelastic plane waves in two and three dimensions are essentially described in terms of the wavevector bivector. This can be written in terms of its real and imaginary parts, representing the real wavenumber vector, and the attenuation vector, respectively. When these vectors coincide in direction, the plane wave is termed homogeneous; when these vectors differ in direction, the plane wave is termed an inhomogeneous body wave. Inhomogeneity has several consequences that make viscoelastic wave behavior particularly different from elastic wave behavior. These behaviors differ mainly in the presence of both inhomogeneities and anisotropy, as we shall see in Chapter 4.

In the geophysical literature, the main contributors to the understanding of wave propagation in isotropic viscoelastic media are Buchen (1971a,b), Borcherdt (1973, 1977, 1982), Borcherdt, Glassmoyer and Wennerberg (1986), and Krebes (1983a,b). The thermodynamical and wave-propagation aspects of the theory are briefly reviewed by Minster (1980) and Chin (1980), respectively. Bland (1960), Beltzer (1988), Christensen (1982), Pipkin (1972), Leitman and Fisher (1984), Caviglia and Morro (1992) and Fabrizio and Morro (1992) provide a rigorous treatment of the subject. In this chapter, we follow the "geophysical" approach to develop the main aspects of the theory of viscoelasticity.

3.1 Stress-strain relation

Let us denote the dimension of the space by n and consider $n = 2$ and $n = 3$ in the following. By $n = 2$ we strictly mean a two-dimensional world and not a plane-strain problem in 3-D space. Therefore, most of the equations lose their tensorial character and should be considered with caution.

The most general isotropic representation of the fourth-order relaxation tensor (2.10) in n-dimensional space is

$$\psi_{ijkl}(t) = \left[\psi_{\mathcal{K}}(t) - \frac{2}{n}\psi_\mu(t)\right]\delta_{ij}\delta_{kl} + \psi_\mu(t)(\delta_{ik}\delta_{jl} + \delta_{il}\delta_{jk}), \tag{3.1}$$

where $\psi_{\mathcal{K}}$ and ψ_μ are independent relaxation functions. Substitution of equation (3.1) into the stress-strain relations (2.9) gives

$$\sigma_{ij} = \left(\psi_{\mathcal{K}} - \frac{2}{n}\psi_\mu\right) * \partial_t\epsilon_{kk}\delta_{ij} + 2\psi_\mu * \partial_t\epsilon_{ij}. \tag{3.2}$$

Taking the trace on both sides of this equation yields

$$\sigma_{ii} = n\psi_{\mathcal{K}} * \partial_t\epsilon_{ii}. \tag{3.3}$$

On the other hand, computing the deviatoric components of stress and strain gives

$$s_{ij} = 2\psi_\mu * \partial_t d_{ij}, \tag{3.4}$$

where

$$s_{ij} = \sigma_{ij} - \frac{1}{n}\sigma_{kk}\delta_{ij} \tag{3.5}$$

and

$$d_{ij} = \epsilon_{ij} - \frac{1}{n}\vartheta\delta_{ij} \tag{3.6}$$

are the components of the deviatoric strain. It is clear that $\psi_{\mathcal{K}}$ describes dilatational deformations, and ψ_μ describes shear deformations; $\psi_{\mathcal{K}}$ is the generalization of the bulk compressibility in the lossless case, and $\psi_{\mathcal{K}} - 2\psi_\mu/n$ and ψ_μ play the role of the Lamé constants λ and μ.

3.2 Equations of motion and dispersion relations

The analysis of wave propagation in homogeneous isotropic media is simplified by the fact that the wave modes are not coupled, as they are in anisotropic media. Applying the divergence operation to equation (1.23), and assuming constant material properties and $f_i = 0$, we obtain

$$\partial_i\partial_j\sigma_{ij} = \rho\partial^2_{tt}\vartheta, \tag{3.7}$$

where

$$\vartheta = \partial_i u_i = \epsilon_{ii} = \mathrm{div}\ \mathbf{u} \tag{3.8}$$

is the dilatation field defined in equation (1.11). Using (3.2), we can write the left-hand side of (3.7) as

$$\partial_t \left(\psi_{\mathcal{K}} - \frac{2}{n}\psi_\mu \right) * \partial_i \partial_i \vartheta + 2\partial_t \psi_\mu * \partial_i \partial_j \epsilon_{ij}. \tag{3.9}$$

Because $2\partial_i \partial_j \epsilon_{ij} = \partial_i \partial_j \partial_j u_i + \partial_i \partial_j \partial_i u_j = 2\partial_i \partial_j \partial_j u_i = 2\partial_i \partial_i \vartheta$ – with the use of (1.2) and (3.8) – we obtain for equation (3.7),

$$\partial_t \left[\psi_{\mathcal{K}} + 2\psi_\mu \left(1 - \frac{1}{n} \right) \right] * \partial_i \partial_i \vartheta = \rho \partial^2_{tt} \vartheta, \tag{3.10}$$

or

$$\partial_t \psi_{\mathcal{E}} * \Delta \vartheta = \rho \partial^2_{tt} \vartheta, \tag{3.11}$$

where $\Delta = \partial_i \partial_i$ is the Laplacian, and

$$\psi_{\mathcal{E}}(t) = \psi_{\mathcal{K}}(t) + 2\psi_\mu(t) \left(1 - \frac{1}{n} \right) \tag{3.12}$$

is the P-wave relaxation function that plays the role of $\lambda + 2\mu$.

Applying the curl operator to equation (1.23), and assuming constant material properties and $f_i = 0$, we obtain

$$\epsilon_{lik} \partial_l \partial_j \sigma_{ij} \hat{\mathbf{e}}_k = \rho \partial^2_{tt} \mathbf{\Omega}, \tag{3.13}$$

where

$$\mathbf{\Omega} = \epsilon_{lik} \partial_l u_i \hat{\mathbf{e}}_k = \text{curl } \mathbf{u} \tag{3.14}$$

and ϵ_{lik} are the components of the Levi-Civita tensor. Substitution of the stress-strain relation (3.2) gives

$$2\partial_t \psi_\mu * \epsilon_{lik} \partial_l \partial_j \epsilon_{ij} \hat{\mathbf{e}}_k = \rho \partial^2_{tt} \mathbf{\Omega}. \tag{3.15}$$

Because $2\epsilon_{lik} \partial_l \partial_j \epsilon_{ij} \ \hat{\mathbf{e}}_k = \epsilon_{lik} \partial_l \partial_j (\partial_i u_j + \partial_j u_i) \ \hat{\mathbf{e}}_k = \epsilon_{lik} \partial_l \partial_i \vartheta \hat{\mathbf{e}}_k + \partial_j \partial_j (\epsilon_{lik} \partial_l u_i) \ \hat{\mathbf{e}}_k = \partial_j \partial_j \mathbf{\Omega}$ (since $\epsilon_{lik} \partial_l \partial_i \vartheta = \text{curl } \vartheta = \text{curl grad } \mathbf{u} = 0$), we finally have

$$\partial_t \psi_\mu * \Delta \mathbf{\Omega} = \rho \partial^2_{tt} \mathbf{\Omega}. \tag{3.16}$$

Fourier transformation of (3.11) and (3.16) to the frequency domain gives the two Helmholtz equations

$$\Delta \vartheta + \frac{\omega^2}{v_P^2} \vartheta = 0, \qquad \Delta \mathbf{\Omega} + \frac{\omega^2}{v_S^2} \mathbf{\Omega} = 0, \tag{3.17}$$

where

$$\rho v_P^2 = \mathcal{F}[\partial_t \psi_{\mathcal{E}}] = \frac{\rho \omega^2}{k_P^2}, \qquad \rho v_S^2 = \mathcal{F}[\partial_t \psi_\mu] = \frac{\rho \omega^2}{k_S^2}, \tag{3.18}$$

with v_P and v_S being the complex and frequency-dependent P-wave and S-wave velocities, and k_P and k_S being the corresponding complex wavenumbers.

The fact that the P- and S-wave modes satisfy equations (3.17) implies that the displacement vector admits the representation

$$\mathbf{u} = \text{grad } \Phi + \text{curl } \mathbf{\Theta}, \qquad \text{div } \mathbf{\Theta} = 0, \tag{3.19}$$

where Φ and $\mathbf{\Theta}$ are a scalar and a vector potential, which satisfy $(3.17)_1$ and $(3.17)_2$, respectively:

$$\Delta\Phi + \frac{\omega^2}{v_P^2}\Phi = 0, \qquad \Delta\mathbf{\Theta} + \frac{\omega^2}{v_S^2}\mathbf{\Theta} = 0. \tag{3.20}$$

These equations can be easily verified by substituting the expression of the displacement into the equation of motion (1.23). The rigorous demonstration for viscoelastic media is given by Edelstein and Gurtin (1965) (cf. Caviglia and Morro, 1992, p. 42).

Let us introduce the complex moduli as in the 1-D case (see equations (2.31), (2.36) and (2.37)),

$$\begin{aligned} \mathcal{K}(\omega) &= \mathcal{F}[\partial_t\psi_{\mathcal{K}}(t)] = \mathcal{K}_R(\omega) + \mathrm{i}\mathcal{K}_I(\omega), \\ \mu(\omega) &= \mathcal{F}[\partial_t\psi_\mu(t)] = \mu_R(\omega) + \mathrm{i}\mu_I(\omega), \end{aligned} \tag{3.21}$$

where

$$\begin{aligned} \mathcal{K}_R(\omega) &= \omega \textstyle\int_0^\infty \breve{\psi}_{\mathcal{K}}(t)\sin(\omega t)dt, \quad & \mathcal{K}_I(\omega) &= \omega \textstyle\int_0^\infty [\breve{\psi}_{\mathcal{K}}(t) - \breve{\psi}_{\mathcal{K}}(0)]\cos(\omega t)dt, \\ \mu_R(\omega) &= \omega \textstyle\int_0^\infty \breve{\psi}_\mu(t)\sin(\omega t)dt, \quad & \mu_I(\omega) &= \omega \textstyle\int_0^\infty [\breve{\psi}_\mu(t) - \breve{\psi}_\mu(0)]\cos(\omega t)dt. \end{aligned} \tag{3.22}$$

Using (3.12) and (3.18), we define $\mathcal{E}$ and μ as

$$\mathcal{E} = \mathcal{F}[\partial_t\psi_{\mathcal{E}}] = \rho v_P^2 = \mathcal{K} + 2\mu\left(1 - \frac{1}{n}\right), \qquad \mu = \rho v_S^2. \tag{3.23}$$

Then, the complex dispersion relations are

$$k_P^2 = \frac{\rho\omega^2}{\mathcal{E}}, \qquad k_S^2 = \frac{\rho\omega^2}{\mu}. \tag{3.24}$$

3.3 Vector plane waves

In general, plane waves in anelastic media have a component of attenuation along the lines of constant phase, meaning that their properties are described by two vectors – the attenuation and propagation vectors, which do not point in the same direction. We analyze in the following sections, the particle motion associated with these vector plane waves.

3.3.1 Slowness, phase velocity and attenuation factor

We consider the viscoelastic plane-wave solution

$$\Phi = \Phi_0 \exp[\mathrm{i}(\omega t - \mathbf{k}\cdot\mathbf{x})], \tag{3.25}$$

where

$$\mathbf{k} = \boldsymbol{\kappa} - \mathrm{i}\boldsymbol{\alpha} = \kappa\hat{\boldsymbol{\kappa}} - \mathrm{i}\alpha\hat{\boldsymbol{\alpha}} \tag{3.26}$$

with $\boldsymbol{\kappa}$ being the real wavevector and $\boldsymbol{\alpha}$ being the attenuation vector. They express the magnitudes of both the wavenumber κ and the attenuation factor α, and the directions of the normals to planes of constant phase and planes of constant amplitude.

Figure 3.1 represents the plane wave (3.25), with γ indicating the inhomogeneity angle. When this angle is zero, the wave is called homogeneous. We note that

$$\mathbf{k} = (\kappa - \mathrm{i}\alpha)\hat{\boldsymbol{\kappa}} \equiv k\hat{\boldsymbol{\kappa}}, \tag{3.27}$$

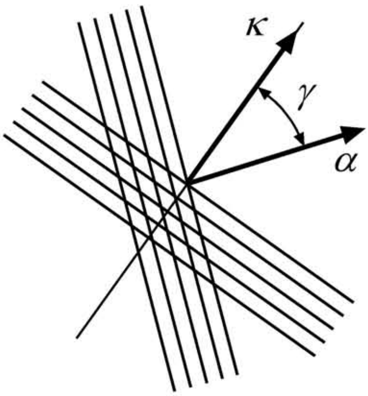

Figure 3.1: Inhomogeneous viscoelastic plane wave. The inhomogeneity angle γ is less than 90°.

only for $\gamma = 0$, i.e., for homogeneous waves. Defining the complex wavenumber

$$k = \frac{\omega}{v_c}, \tag{3.28}$$

where v_c is the complex velocity defined in (3.18), the wavenumber and the attenuation factor for homogeneous waves have the simple form

$$\kappa_H = \omega \mathrm{Re}\left(\frac{1}{v_c}\right) \tag{3.29}$$

and

$$\alpha_H = -\omega \mathrm{Im}\left(\frac{1}{v_c}\right), \tag{3.30}$$

as in the 1-D case (see equations (2.83) and (2.85)). Substitution of the plane-wave solution (3.25) into equation $(3.20)_1$, and the use of $(3.18)_1$ yields

$$\mathbf{k} \cdot \mathbf{k} = k_P^2 = k^2 = \mathrm{Re}(k^2)(1 - \mathrm{i}Q_H^{-1}), \tag{3.31}$$

where

$$Q_H = -\frac{\mathrm{Re}(k^2)}{\mathrm{Im}(k^2)} \tag{3.32}$$

is the quality factor for homogeneous plane waves (Section 3.4.1). This quantity is an intrinsic property of the medium. For inhomogeneous plane waves, the quality factor also depends on the inhomogeneity angle γ, which is a characteristic of the wave field. Separating real and imaginary parts in equation (3.31), we have

$$\begin{aligned} \kappa^2 - \alpha^2 &= \mathrm{Re}(k^2), \\ 2\kappa\alpha \cos\gamma &= -\mathrm{Im}(k^2) = \mathrm{Re}(k^2) Q_H^{-1}. \end{aligned} \tag{3.33}$$

Solving for κ and α, we obtain

$$
\begin{aligned}
2\kappa^2 &= \mathrm{Re}(k^2) + \sqrt{[\mathrm{Re}(k^2)]^2 + [\mathrm{Im}(k^2)]^2 \sec^2\gamma}, \\
2\alpha^2 &= -\mathrm{Re}(k^2) + \sqrt{[\mathrm{Re}(k^2)]^2 + [\mathrm{Im}(k^2)]^2 \sec^2\gamma},
\end{aligned}
\tag{3.34}
$$

or,

$$
\begin{aligned}
2\kappa^2 &= \mathrm{Re}(k^2)\left(1 + \sqrt{1 + Q_H^{-2}\sec^2\gamma}\right), \\
2\alpha^2 &= \mathrm{Re}(k^2)\left(-1 + \sqrt{1 + Q_H^{-2}\sec^2\gamma}\right).
\end{aligned}
\tag{3.35}
$$

We first note that if $\mathrm{Im}(k^2) = 0$ ($Q_H \to \infty$), $\alpha = 0$, and $\gamma = \pi/2$. This case corresponds to an inhomogeneous elastic wave propagating in a lossless material, generated by refraction, for instance. In a lossy material, γ must satisfy

$$
0 \leq \gamma < \pi/2. \tag{3.36}
$$

We may include the case $\gamma = \pi/2$, keeping in mind that this case corresponds to the limit of a lossless medium.

The phase-velocity and slowness vectors for inhomogeneous plane waves are

$$
\mathbf{v}_p = \left(\frac{\omega}{\kappa}\right)\hat{\boldsymbol{\kappa}}, \quad \mathbf{s}_R = \left(\frac{\kappa}{\omega}\right)\hat{\boldsymbol{\kappa}}, \tag{3.37}
$$

and the attenuation vector $\boldsymbol{\alpha}$ is implicitly defined in (3.26). For homogeneous plane waves, equation (3.29) implies

$$
\mathbf{v}_{pH} = \left[\mathrm{Re}\left(\frac{1}{v_c}\right)\right]^{-1}\hat{\boldsymbol{\kappa}}, \quad \mathbf{s}_{RH} = \omega \mathrm{Re}\left(\frac{1}{v_c}\right)\hat{\boldsymbol{\kappa}}, \tag{3.38}
$$

where v_c represents the P-wave velocity v_P defined in $(3.18)_1$. We can infer, from equations (3.35) and $(3.37)_1$, that the phase velocity and attenuation factor of an inhomogeneous plane wave tend to zero and ∞, respectively, as γ approaches $\pi/2$, and that they are less than and greater than the corresponding quantities for homogeneous plane waves.

3.3.2 Particle motion of the P wave

Equation (3.19) implies that the P-wave displacement vector can be expressed in terms of the scalar potential (3.25) as

$$
\mathbf{u} = \mathrm{grad}\ \Phi = \mathrm{Re}\{-\mathrm{i}\Phi_0 \mathbf{k} \exp[\mathrm{i}(\omega t - \mathbf{k}\cdot\mathbf{x})]\}. \tag{3.39}
$$

Using equation (3.26) and $\Phi_0 k = |\Phi_0 k| \exp[\mathrm{i}\ \arg(\Phi_0 k)]$, we obtain

$$
\mathbf{u} = -|\Phi_0 k| \exp(-\boldsymbol{\alpha}\cdot\mathbf{x})\ \mathrm{Re}\left[\mathrm{i}\left(\frac{v_c}{\omega}\right)\mathbf{k}\exp(\mathrm{i}\varsigma)\right], \tag{3.40}
$$

where

$$
\varsigma(t) = \omega t - \boldsymbol{\kappa}\cdot\mathbf{x} + \arg(\Phi_0 k). \tag{3.41}
$$

Equation (3.28) has been used (v_c represents the P-wave complex velocity v_P defined in equation $(3.18)_1$). We introduce the real vectors $\boldsymbol{\xi}_1$ and $\boldsymbol{\xi}_2$, such that

$$
\left(\frac{v_c}{\omega}\right)\mathbf{k} = \left(\frac{v_c}{\omega}\right)(\boldsymbol{\kappa} - \mathrm{i}\boldsymbol{\alpha}) = \boldsymbol{\xi}_1 + \mathrm{i}\boldsymbol{\xi}_2 \tag{3.42}
$$

where

$$\omega \boldsymbol{\xi}_1 = v_R \boldsymbol{\kappa} + v_I \boldsymbol{\alpha}, \qquad \omega \boldsymbol{\xi}_2 = v_I \boldsymbol{\kappa} - v_R \boldsymbol{\alpha}, \tag{3.43}$$

and v_R and v_I denote the real and imaginary parts of v_c. Now,

$$\omega^2 \boldsymbol{\xi}_1 \cdot \boldsymbol{\xi}_2 = v_I v_R (\kappa^2 - \alpha^2) + (v_I^2 - v_R^2) \boldsymbol{\kappa} \cdot \boldsymbol{\alpha}, \tag{3.44}$$

which, using equations (3.28) and (3.33), implies

$$\boldsymbol{\xi}_1 \cdot \boldsymbol{\xi}_2 = v_I v_R \mathrm{Re}\left(\frac{1}{v_c^2}\right) + \frac{1}{2}(v_I^2 - v_R^2)\mathrm{Im}\left(\frac{1}{v_c^2}\right) \propto v_I v_R \mathrm{Re}(v_c^{2^*}) + \frac{1}{2}\mathrm{Im}(v_c^{2^*})(v_I^2 - v_R^2) = 0. \tag{3.45}$$

Thus, the vectors are orthogonal,

$$\boldsymbol{\xi}_1 \cdot \boldsymbol{\xi}_2 = 0. \tag{3.46}$$

Moreover,

$$\omega^2 (\xi_1^2 - \xi_2^2) = (\kappa^2 - \alpha^2)(v_R^2 - v_I^2) + 4 v_R v_I (\boldsymbol{\kappa} \cdot \boldsymbol{\alpha}). \tag{3.47}$$

Again, using equations (3.28) and (3.33), we obtain

$$\begin{aligned} \xi_1^2 - \xi_2^2 &= \mathrm{Re}\left(\frac{1}{v_c^2}\right)(v_R^2 - v_I^2) - 2 v_R v_I \mathrm{Im}\left(\frac{1}{v_c^2}\right) \\ &= \frac{1}{|v_c|^4}[(v_R^2 - v_I^2)^2 + 4 v_R^2 v_I^2] = \frac{1}{|v_c|^4}(v_R^2 + v_I^2)^2 = 1; \end{aligned} \tag{3.48}$$

that is

$$\xi_1^2 - \xi_2^2 = 1. \tag{3.49}$$

Since $\xi_1 > 0$ and $\xi_2 > 0$, equation (3.49) implies $\xi_1 > \xi_2$. Substitution of equation (3.42) into equation (3.40) gives

$$\mathbf{u} = -|\Phi_0 k| \exp(-\boldsymbol{\alpha} \cdot \mathbf{x}) \mathrm{Re}\left[\mathrm{i}(\boldsymbol{\xi}_1 + \mathrm{i}\boldsymbol{\xi}_2) \exp(\mathrm{i}\varsigma)\right], \tag{3.50}$$

or

$$\mathbf{u} = U_0 [\boldsymbol{\xi}_1 \sin\varsigma + \boldsymbol{\xi}_2 \cos\varsigma], \tag{3.51}$$

with

$$U_0 = |\Phi_0 k| \exp(-\boldsymbol{\alpha} \cdot \mathbf{x}). \tag{3.52}$$

We write the following definition:

$$U_1 = \frac{\mathbf{u} \cdot \boldsymbol{\xi}_1}{\xi_1 U_0}, \qquad U_2 = -\frac{\mathbf{u} \cdot \boldsymbol{\xi}_2}{\xi_2 U_0}, \tag{3.53}$$

and eliminate ς from (3.51) to obtain

$$\frac{U_1^2}{\xi_1^2} + \frac{U_2^2}{\xi_2^2} = 1. \tag{3.54}$$

Equation (3.54) indicates that the particle motion is an ellipse, with major axis $\boldsymbol{\xi}_1$ and minor axis $\boldsymbol{\xi}_2$. The sense of rotation is from $\boldsymbol{\kappa}$ to $\boldsymbol{\alpha}$ and the plane of motion is defined by these vectors (see Figure 3.2). The cosine of the angle between the propagation direction and the major axis of the ellipse is given by $\boldsymbol{\kappa} \cdot \boldsymbol{\xi}_1 / (\kappa \xi_1)$.

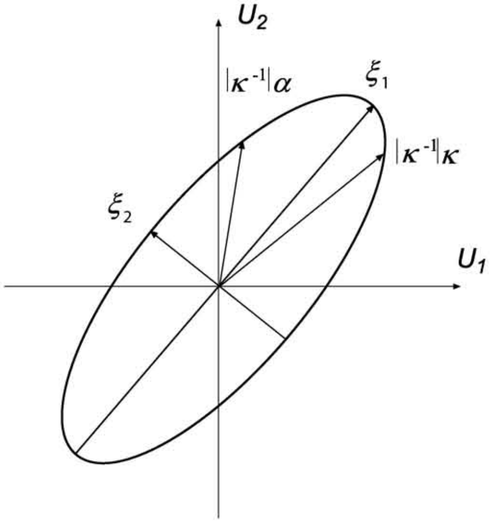

Figure 3.2: Particle motion of an inhomogeneous P wave in an isotropic viscoelastic medium. The ellipse degenerates into a straight line for a homogeneous plane wave.

This means that the particle motion of an inhomogeneous plane P wave is not purely longitudinal. When $\gamma = 0$ (i.e., an homogeneous plane wave),

$$\omega \boldsymbol{\xi}_2 = \hat{\boldsymbol{\kappa}}(v_I \kappa - v_R \alpha), \tag{3.55}$$

according to equations (3.27) and $(3.43)_2$. But from equations (3.29) and (3.30), we have

$$v_I \kappa - v_R \alpha = v_I \kappa_H - v_R \alpha_H = \omega \left[v_I \mathrm{Re}\left(\frac{1}{v_c}\right) + v_R \mathrm{Im}\left(\frac{1}{v_c}\right)\right] = 0. \tag{3.56}$$

Hence, $\xi_2 = 0$, and the particle motion is longitudinal.

3.3.3 Particle motion of the S waves

We can define two types of S waves, depending on the location of the particle motion, with respect to the $(\boldsymbol{\kappa}, \boldsymbol{\alpha})$-plane. Let us consider a plane-wave solution for type-I S waves of the form

$$\boldsymbol{\Theta} = \mathrm{Re}\{\Theta_0 \hat{\mathbf{n}} \exp[\mathrm{i}(\omega t - \mathbf{k} \cdot \mathbf{x})]\}, \tag{3.57}$$

where Θ_0 is a complex constant and $\hat{\mathbf{n}}$ is a unit vector perpendicular to the $(\boldsymbol{\kappa}, \boldsymbol{\alpha})$-plane. This is a consequence of equation $(3.19)_2$, which implies $\mathbf{k} \cdot \hat{\mathbf{n}} = 0$. Orthogonality, in this case, should be understood in the sense of complex vectors (see Caviglia and Morro, 1992, p. 8, 46), and the condition $\mathbf{k} \cdot \hat{\mathbf{n}} = 0$ does not imply that the polarization $\mathrm{Re}(\mathbf{u})$ (see equation (3.60) below) is perpendicular to the real wavenumber vector $\boldsymbol{\kappa}$.

The solution for type-II S waves is obtained by considering a plane wave,

$$\boldsymbol{\Theta} = \mathrm{Re}\{(\theta_1 \hat{\mathbf{e}}_1 + \theta_3 \hat{\mathbf{e}}_3) \exp[\mathrm{i}(\omega t - \mathbf{k} \cdot \mathbf{x})]\}, \tag{3.58}$$

with θ_1 and θ_3 being complex valued. Moreover, let us assume that the $(\boldsymbol{\kappa}, \boldsymbol{\alpha})$-plane coincides with the (x, z)-plane, implying $\partial_2[\,\cdot\,] = 0$. From equation $(3.19)_1$, the displacement field for such a wave is given by

$$\mathbf{u} = \mathrm{Re}\{\Gamma_0 \exp[\mathrm{i}(\omega t - \mathbf{k} \cdot \mathbf{x})]\}\hat{\mathbf{e}}_2, \qquad \Gamma_0 = (\theta_3 \hat{\mathbf{e}}_1 - \theta_1 \hat{\mathbf{e}}_3) \cdot (\boldsymbol{\alpha} + \mathrm{i}\boldsymbol{\kappa}), \tag{3.59}$$

and $(3.19)_2$ implies $\theta_1(\boldsymbol{\alpha} + \mathrm{i}\boldsymbol{\kappa}) \cdot \hat{\mathbf{e}}_1 = -\theta_3(\boldsymbol{\alpha} + \mathrm{i}\boldsymbol{\kappa}) \cdot \hat{\mathbf{e}}_3$. Equation (3.59) indicates that the particle motion is linear perpendicular to the $(\boldsymbol{\kappa}, \boldsymbol{\alpha})$-plane.

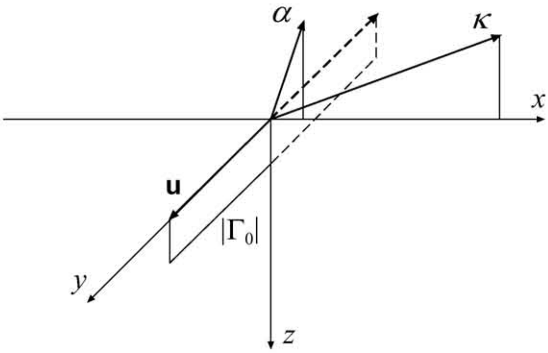

Figure 3.3: Linear particle motion of a type-II S wave (SH wave).

Figure 3.3 shows the particle motion of the type-II S wave. Type-I and type-II S waves are denoted by the symbols SV and SH in seismology (Buchen, 1971a,b; Borcherdt, 1977).

The particle motion of the type-I S wave shows similar characteristics to the P-wave particle motion. From (3.19), its displacement vector can be expressed in terms of vector $\boldsymbol{\Theta}$ as

$$\mathbf{u} = \mathrm{curl}\ \boldsymbol{\Theta} = \mathrm{Re}\{-\mathrm{i}\Theta_0(\hat{\mathbf{n}} \times \mathbf{k}) \exp[\mathrm{i}(\omega t - \mathbf{k} \cdot \mathbf{x})]\}, \tag{3.60}$$

which lies in the plane of $\boldsymbol{\kappa}$ and $\boldsymbol{\alpha}$.

For simplicity, we use the same notation as for the P wave, but the complex velocity v_c is equal here to v_S, defined in $(3.18)_2$. Using equation (3.26) and $\Theta_0 k = |\Theta_0 k| \exp[\mathrm{i}\ \arg(\Theta_0 k)]$, we get

$$\mathbf{u} = -|\Theta_0 k| \exp(-\boldsymbol{\alpha} \cdot \mathbf{x}) \mathrm{Re}\left[\mathrm{i}\left(\frac{v_c}{\omega}\right)(\hat{\mathbf{n}} \times \mathbf{k}) \exp(\mathrm{i}\varsigma)\right], \tag{3.61}$$

where

$$\varsigma(t) = \omega t - \boldsymbol{\kappa} \cdot \mathbf{x} + \arg(\Theta_0 k). \tag{3.62}$$

As before, $v_c \mathbf{k}/\omega$ can be decomposed into real and imaginary vectors as in equation (3.42). Let us define

$$\left(\frac{v_c}{\omega}\right) \hat{\mathbf{n}} \times \mathbf{k} = \boldsymbol{\zeta}_1 + \mathrm{i}\boldsymbol{\zeta}_2, \tag{3.63}$$

where

$$\boldsymbol{\zeta}_1 = \hat{\mathbf{n}} \times \boldsymbol{\xi}_1, \qquad \boldsymbol{\zeta}_2 = \hat{\mathbf{n}} \times \boldsymbol{\xi}_2, \tag{3.64}$$

since $\boldsymbol{\xi}_1$ and $\boldsymbol{\xi}_2$, defined in equation (3.43), lie in the $(\boldsymbol{\kappa}, \boldsymbol{\alpha})$-plane. On the basis of equations (3.46), (3.49) and (3.64), these vectors have the properties

$$\boldsymbol{\zeta}_1 \cdot \boldsymbol{\zeta}_2 = 0, \quad \zeta_1^2 - \zeta_2^2 = 1. \tag{3.65}$$

Substituting (3.63) into equation (3.61) gives

$$\mathbf{u} = U_0[\boldsymbol{\zeta}_1 \sin \varsigma + \boldsymbol{\zeta}_2 \cos \varsigma], \tag{3.66}$$

with

$$U_0 = |\Theta_0 k| \exp(-\boldsymbol{\alpha} \cdot \mathbf{x}). \tag{3.67}$$

The particle motion is an ellipse, whose major and minor axes are given by $\boldsymbol{\zeta}_1$ and $\boldsymbol{\zeta}_2$, and whose direction of rotation is from $\boldsymbol{\kappa}$ to $\boldsymbol{\alpha}$. The cosine of the angle between the propagation direction and the major axis of the ellipse is given by $\boldsymbol{\kappa} \cdot \boldsymbol{\zeta}_1/(\kappa\zeta_1)$ (Buchen, 1971a).

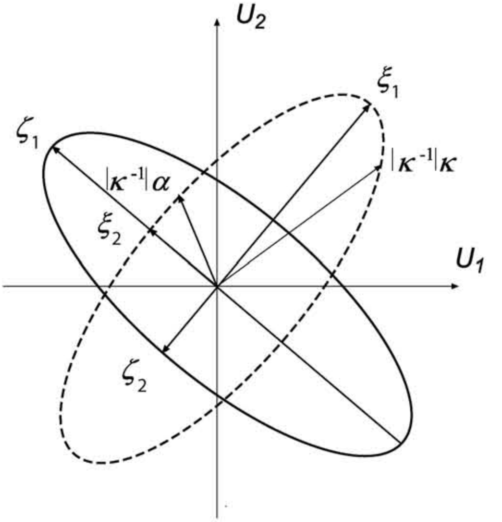

Figure 3.4: Particle motion of an inhomogeneous S wave in an isotropic viscoelastic medium. The ellipse degenerates into a straight line for a homogeneous plane wave.

Figure 3.4 shows a diagram of the S-wave particle motion. For a homogeneous plane wave, the ellipse degenerates into a straight line.

3.3.4 Polarization and orthogonality

We have seen in Section 1.3.3 that the polarizations of the three wave modes are orthogonal in anisotropic elastic media. Now, consider the case of anelastic isotropic media. From equations (3.40) and (3.61), the P and S-I polarizations have the form

$$\mathbf{u}_{\mathrm{P}} = \mathrm{Re}[a(\boldsymbol{\kappa}_{\mathrm{P}} - \mathrm{i}\boldsymbol{\alpha}_{\mathrm{P}})] \quad \text{and} \quad \mathbf{u}_{\mathrm{S}} = \mathrm{Re}(b\hat{\mathbf{n}} \times (\boldsymbol{\kappa}_{\mathrm{S}} - \mathrm{i}\boldsymbol{\alpha}_{\mathrm{S}})], \tag{3.68}$$

respectively, where a and b are complex quantities, and the indices P and S indicate that $\boldsymbol{\kappa}$ and $\boldsymbol{\alpha}$ for P and S waves differ. The general form (3.68) implies that the P and S polarizations are not orthogonal in general, that is, when the plane waves are inhomogeneous. For homogeneous waves, $\hat{\boldsymbol{\alpha}} = \hat{\boldsymbol{\kappa}}$, and if the propagation directions coincide, equation (3.68) simplifies to

$$\mathbf{u}_{\mathrm{P}} = \mathrm{Re}(a')\ \hat{\boldsymbol{\kappa}} \quad \text{and} \quad \mathbf{u}_{\mathrm{S}} = \mathrm{Re}(b')\ \hat{\mathbf{n}} \times \hat{\boldsymbol{\kappa}}, \tag{3.69}$$

where a' and b' are complex quantities. These two vectors are orthogonal, since $\hat{\mathbf{n}}$ is perpendicular to $\hat{\boldsymbol{\kappa}}$.

3.4 Energy balance, energy velocity and quality factor

To derive the mechanical energy-balance equation, we follow the same steps as we did to obtain equation (2.95) in the 1-D case. Using $\partial_t u_i = v_i$ ($\partial_t \mathbf{u} = \mathbf{v}$) and performing the scalar product of equation (1.23) with $\mathbf{v}$ on both sides, we get

$$v_i \partial_j \sigma_{ij} = \rho v_i \partial_t v_i, \tag{3.70}$$

where we assumed $f_i = 0$. Contraction of $\partial_j v_i + \partial_i v_j = 2\partial_t \epsilon_{ij}$ with σ_{ij} yields

$$\sigma_{ij} \partial_t \epsilon_{ij} = \frac{1}{2} \sigma_{ij} (\partial_j v_i + \partial_i v_j) = \sigma_{ij} \partial_j v_i, \tag{3.71}$$

using the symmetry of the stress tensor. Adding equations (3.70) and (3.71) and substituting the stress-strain relation (3.2), we obtain the energy-balance equation, equivalent to (2.94),

$$-\partial_i p_i = \partial_t T + \left[\left(\partial_t \psi_K - \frac{2}{n} \partial_t \psi_\mu \right) * \epsilon_{kk} \delta_{ij} + 2\partial_t \psi_\mu * \epsilon_{ij} \right] \partial_t \epsilon_{ij}, \tag{3.72}$$

where

$$p_i = -v_j \sigma_{ij} \tag{3.73}$$

are the components of the Umov-Poynting vector, and

$$T = \frac{1}{2} \rho v_i v_i \tag{3.74}$$

is the kinetic-energy density.

The second term in the right-hand side is then partitioned in terms of the rate of strain and dissipated energies on the basis of expressions (2.16) and (2.17). We obtain

$$-\mathrm{div}\ \mathbf{p} = \partial_t (T + V) + \dot{D}, \tag{3.75}$$

where, defining $\tau' = 2t - \tau_1 - \tau_2$ and using (3.1), we have that the strain energy is

$$V(t) = \frac{1}{2} \int_{-\infty}^{t} \int_{-\infty}^{t} \left\{ \left[\breve{\psi}_K(\tau') - \frac{2}{n} \breve{\psi}_\mu(\tau') \right] \delta_{ij} \delta_{kl} + \breve{\psi}_\mu(\tau') (\delta_{ik} \delta_{jl} + \delta_{il} \delta_{jk}) \right\}$$

$$\partial_{\tau_1}\epsilon_{ij}(\tau_1)\partial_{\tau_2}\epsilon_{kl}(\tau_2)d\tau_1 d\tau_2. \tag{3.76}$$

Equation (3.76) becomes

$$V(t) = \frac{1}{2}\int_{-\infty}^{t}\int_{-\infty}^{t} \breve{\psi}_K(\tau')\partial_{\tau_1}\epsilon_{ii}(\tau_1)\partial_{\tau_2}\epsilon_{kk}(\tau_2)d\tau_1 d\tau_2$$

$$+\int_{-\infty}^{t}\int_{-\infty}^{t} \breve{\psi}_\mu(\tau')\left[\partial_{\tau_1}\epsilon_{ij}(\tau_1)\partial_{\tau_2}\epsilon_{ij}(\tau_2) - \frac{1}{n}\partial_{\tau_1}\epsilon_{ii}(\tau_1)\partial_{\tau_2}\epsilon_{kk}(\tau_2)\right] d\tau_1 d\tau_2, \tag{3.77}$$

where we used the symmetry of the strain tensor. In terms of the deviatoric components of strain (3.6), equation (3.77) becomes

$$V(t) = \frac{1}{2}\int_{-\infty}^{t}\int_{-\infty}^{t} \breve{\psi}_K(\tau')\partial_{\tau_1}\epsilon_{ii}(\tau_1)\partial_{\tau_2}\epsilon_{kk}(\tau_2)d\tau_1 d\tau_2$$

$$+\int_{-\infty}^{t}\int_{-\infty}^{t} \breve{\psi}_\mu(\tau')\partial_{\tau_1}d_{ij}(\tau_1)\partial_{\tau_2}d_{ij}(\tau_2)d\tau_1 d\tau_2. \tag{3.78}$$

To obtain the last equation, we must be careful with terms of the form $\partial_{\tau_1}\epsilon_{ij}\partial_{\tau_2}\epsilon_{ij}$, when $i \neq j$, since they come in pairs; e.g., $\partial_{\tau_1}\epsilon_{12}(\tau_1)\partial_{\tau_2}\epsilon_{12}(\tau_2)+ \partial_{\tau_1}\epsilon_{21}(\tau_1)\partial_{\tau_2}\epsilon_{21}(\tau_2) = 2\partial_{\tau_1}\epsilon_{12}(\tau_1)\partial_{\tau_2}\epsilon_{12}(\tau_2)$.

Similarly, the rate of dissipated-energy density can be expressed as

$$\dot{D}(t) = -\int_{-\infty}^{t}\int_{-\infty}^{t} \partial\breve{\psi}_K(\tau')\partial_{\tau_1}\epsilon_{ii}(\tau_1)\partial_{\tau_2}\epsilon_{kk}(\tau_2)d\tau_1 d\tau_2$$

$$-\int_{-\infty}^{t}\int_{-\infty}^{t} 2\partial\breve{\psi}_\mu(\tau')\partial_{\tau_1}d_{ij}(\tau_1)\partial_{\tau_2}d_{ij}(\tau_2)d\tau_1 d\tau_2, \tag{3.79}$$

where ∂ denotes the derivative with respect to the argument.

3.4.1 P wave

In this section, we obtain the mechanical energy-balance equation for P waves. The complex displacement and particle-velocity components are from (3.39)

$$u_i = -\mathrm{i}\Phi_0 k_i \exp[\mathrm{i}(\omega t - \mathbf{k}\cdot\mathbf{x})] \tag{3.80}$$

and

$$v_i = \partial_t u_i = \omega\Phi_0 k_i \exp[\mathrm{i}(\omega t - \mathbf{k}\cdot\mathbf{x})], \tag{3.81}$$

with $k = k_P$ in this case.

The time-averaged kinetic-energy density (3.74) can be easily calculated by using equation (1.105),

$$\langle T\rangle = \frac{1}{4}\rho\mathrm{Re}(v_i v_i^*) = \frac{1}{4}\rho|\mathbf{v}|^2 = \frac{1}{4}\rho\omega^2|\Phi_0|^2(\mathbf{k}\cdot\mathbf{k}^*)\exp(-2\boldsymbol{\alpha}\cdot\mathbf{x})$$

$$= \frac{1}{4}\rho\omega^2|\Phi_0|^2\exp(-2\boldsymbol{\alpha}\cdot\mathbf{x})(|\boldsymbol{\kappa}|^2 + |\boldsymbol{\alpha}|^2), \tag{3.82}$$

where equation (3.26) was used. By virtue of (3.34), we can recast the kinetic-energy density in terms of the inhomogeneity angle γ,

$$\langle T\rangle = \frac{1}{4}\rho\omega^2|\Phi_0|^2\exp(-2\boldsymbol{\alpha}\cdot\mathbf{x})\sqrt{[\mathrm{Re}(k^2)]^2+[\mathrm{Im}(k^2)]^2\sec^2\gamma}. \tag{3.83}$$

Let us now consider the strain-energy density (3.78). From equations (3.19) and (3.25), we have

$$\partial_t\epsilon_{ii} = \partial_i v_i = -\mathrm{i}\omega k^2\Phi \tag{3.84}$$

and

$$\partial_t d_{ij} = -\mathrm{i}\omega\left(k_ik_j - \frac{1}{n}\delta_{ij}k^2\right)\Phi. \tag{3.85}$$

Since $\tau' = 2t-\tau_1-\tau_2$, the change of variables $\tau_1 \to t-\tau_1$ and $\tau_2 \to t-\tau_2$ in equation (3.78) yields

$$V(t) = \frac{1}{2}\int_0^\infty\int_0^\infty \breve{\psi}_{\mathcal{K}}(\tau_1+\tau_2)\partial\epsilon_{ii}(t-\tau_1)\partial\epsilon_{kk}(t-\tau_2)d\tau_1d\tau_2$$
$$+\int_0^\infty\int_0^\infty \breve{\psi}_{\mu}(\tau_1+\tau_2)\partial d_{ij}(t-\tau_1)\partial d_{ij}(t-\tau_2)d\tau_1d\tau_2. \tag{3.86}$$

Averaging over a period $2\pi/\omega$ by using (1.105), we note that

$$\langle\partial\epsilon_{ii}(t-\tau_1)\partial\epsilon_{kk}(t-\tau_2)\rangle = \frac{1}{2}\mathrm{Re}\{\partial\epsilon_{ii}(t-\tau_1)[\partial\epsilon_{kk}(t-\tau_2)]^*\} = \frac{1}{2}\omega^2|k|^4|\Phi|^2\cos[\omega(\tau_2-\tau_1)], \tag{3.87}$$

where equation (3.84) has been used. Similarly, using (3.85), we obtain

$$\langle\partial d_{ij}(t-\tau_1)\partial d_{ij}(t-\tau_2)\rangle = \frac{1}{2}\omega^2\left|k_ik_j-\frac{1}{n}\delta_{ij}k^2\right|^2|\Phi|^2\cos[\omega(\tau_2-\tau_1)], \tag{3.88}$$

where implicit summation is assumed in the square of the absolute modulus. Now, by a new change of variables similar to the one used to obtain equation (2.47), we have

$$\langle V\rangle = \frac{1}{4}\omega|k|^4|\Phi|^2\int_0^\infty \breve{\psi}_{\mathcal{K}}\sin(\omega\zeta)d\zeta + \frac{1}{2}\omega\left|k_ik_j-\frac{1}{n}\delta_{ij}k^2\right|^2|\Phi|^2\int_0^\infty\breve{\psi}_\mu\sin(\omega\zeta)d\zeta. \tag{3.89}$$

Substituting the expressions of the real moduli (3.22) into equation (3.89), we obtain

$$\langle V\rangle = \frac{1}{4}|\Phi_0|^2\exp(-2\boldsymbol{\alpha}\cdot\mathbf{x})\left(|k|^4\mathcal{K}_R + 2\left|k_ik_j-\frac{1}{n}\delta_{ij}k^2\right|^2\mu_R\right), \tag{3.90}$$

where equations (3.25) and (3.26) were used. But,

$$\begin{aligned}
\left|k_ik_j-\tfrac{1}{n}\delta_{ij}k^2\right|^2 &= (k_ik_j-\tfrac{1}{n}\delta_{ij}k^2)(k_i^*k_j^*-\tfrac{1}{n}\delta_{ij}k^{2*})\\
&= (\mathbf{k}\cdot\mathbf{k}^*)^2-\tfrac{1}{n}k^2k^{2*}\\
&= (\kappa^2+\alpha^2)^2-\tfrac{1}{n}|k^2|^2\\
&= [\mathrm{Re}(k^2)]^2+[\mathrm{Im}(k^2)]^2\sec^2\gamma-\tfrac{1}{n}\{[\mathrm{Re}(k^2)]^2+[\mathrm{Im}(k^2)]^2\}\\
&= \{[\mathrm{Re}(k^2)]^2+[\mathrm{Im}(k^2)^2]\}\left(1-\tfrac{1}{n}\right)+[\mathrm{Im}(k^2)]^2\tan^2\gamma,
\end{aligned} \tag{3.91}$$

where we have used (3.24) and (3.34). Substituting expression (3.91) into equation (3.90), we have

$$\langle V\rangle = \frac{1}{4}|\Phi_0|^2 \exp(-2\boldsymbol{\alpha}\cdot\mathbf{x})\left\{\{[\mathrm{Re}(k^2)]^2+[\mathrm{Im}(k^2)]^2\}\left[\mathcal{K}_R+\left(2-\frac{2}{n}\right)\mu_R\right]\right.$$
$$\left. +2\mu_R[\mathrm{Im}(k^2)\tan\gamma]^2\right\}. \tag{3.92}$$

From equation (3.23),

$$\mathcal{K}_R+\left(2-\frac{2}{n}\right)\mu_R = \mathrm{Re}(\mathcal{E}) = \frac{\rho\omega^2\mathrm{Re}(k^2)}{[\mathrm{Re}(k^2)]^2+[\mathrm{Im}(k^2)]^2}, \tag{3.93}$$

such that (3.92) becomes

$$\langle V\rangle = \frac{1}{4}|\Phi_0|^2 \exp(-2\boldsymbol{\alpha}\cdot\mathbf{x})\{\rho\omega^2\mathrm{Re}(k^2)+2\mu_R[\mathrm{Im}(k^2)\tan\gamma]^2\}, \tag{3.94}$$

where k must be replaced by k_P. This can be written in terms of the medium properties by using equation (3.24). Expression (3.94) is obtained by Buchen (1971a).

Note, from equation (3.33), that

$$\mathrm{Re}(k^2) = \kappa^2-\alpha^2 \tag{3.95}$$

and

$$[\mathrm{Im}(k^2)\tan\gamma]^2 = 4\kappa^2\alpha^2\sin^2\gamma = 4|\boldsymbol{\kappa}\times\boldsymbol{\alpha}|^2. \tag{3.96}$$

Therefore, equation (3.94) can be rewritten as

$$\langle V\rangle = \frac{1}{4}|\Phi_0|^2 \exp(-2\boldsymbol{\alpha}\cdot\mathbf{x})[\rho\omega^2(|\boldsymbol{\kappa}|^2-|\boldsymbol{\alpha}|^2)+8\mu_R|\boldsymbol{\kappa}\times\boldsymbol{\alpha}|^2]. \tag{3.97}$$

This form is obtained by Borcherdt (1973), but with the factor 4 in the second term, instead of the factor 8. This and other discrepancies have given rise to a discussion between Krebes (1983a) and Borcherdt (see Borcherdt and Wennerberg, 1985) regarding the preferred definitions of strain and dissipated energies. As pointed out by Caviglia and Morro (1992, p. 57), in the general case, the ambiguities remain, even though the time averages are considered. We should emphasize, however, that the ambiguity disappears when we consider energy densities compatible with mechanical models of viscoelastic behavior, as in the approach followed by Buchen (1971a). This discrepancy does not occur for homogeneous waves, because $\boldsymbol{\kappa}\times\boldsymbol{\alpha}=0$, but may have implications when calculating the reflection and transmission coefficients at discontinuities, since inhomogeneous waves are generated.

The same procedure can be used to obtain the time-averaged rate of dissipated-energy density. (The reader may try to obtain the expression as an exercise). A detailed demonstration is given by Buchen (1971a):

$$\langle\dot{D}\rangle = \frac{1}{2}\omega|\Phi_0|^2\exp(-2\boldsymbol{\alpha}\cdot\mathbf{x})\mathrm{Im}(k^2)[-\rho\omega^2+2\mu_I\mathrm{Im}(k^2)\tan^2\gamma], \tag{3.98}$$

or, in terms of the wavenumber and attenuation vectors, time-averaged dissipated-energy density is

$$\langle D\rangle = |\Phi_0|^2\exp(-2\boldsymbol{\alpha}\cdot\mathbf{x})[\rho\omega^2(\boldsymbol{\kappa}\cdot\boldsymbol{\alpha})+4\mu_I|\boldsymbol{\kappa}\times\boldsymbol{\alpha}|^2], \tag{3.99}$$

where we have used equations (2.106), $(3.33)_2$ and (3.96).

We now note the following properties. Since $\langle V \rangle$ in (3.97) must be a positive definite quantity, it follows that $\mathrm{Re}(k_P^2) > 0$, and from (3.24),

$$\mathrm{Re}(\mathcal{E}) = \mathcal{E}_R > 0. \tag{3.100}$$

In addition,

$$\mu_R > 0. \tag{3.101}$$

Also, since $\langle \dot{D} \rangle$ must be non-negative, it follows that $\mathrm{Im}(k_P^2) < 0$ – this can also be deduced from (3.33), since $\boldsymbol{\kappa} \cdot \boldsymbol{\alpha} > 0$ – or

$$\mathrm{Im}(\mathcal{E}) = \mathcal{E}_I > 0, \tag{3.102}$$

according to (3.24). Furthermore, since $\boldsymbol{\kappa} \cdot \boldsymbol{\alpha} > 0$,

$$\mu_I > 0. \tag{3.103}$$

The time average of the total energy density, from (3.82) and (3.97), is

$$\langle E \rangle = \langle T + V \rangle = \frac{1}{2}|\Phi_0|^2 \exp(-2\boldsymbol{\alpha} \cdot \mathbf{x})[\rho\omega^2|\boldsymbol{\kappa}|^2 + 4\mu_R|\boldsymbol{\kappa} \times \boldsymbol{\alpha}|^2]. \tag{3.104}$$

When the motion is lossless ($\mathrm{Im}(k_P^2) = 0$), the time-averaged kinetic- and strain-energy densities are the same

$$\langle T \rangle = \langle V \rangle = \frac{1}{4}|\Phi_0|^2 \exp(-2\boldsymbol{\alpha} \cdot \mathbf{x})\rho\omega^2 k_P^2. \tag{3.105}$$

Let us calculate now the time-averaged energy flow, or the time average of the Umov-Poynting vector. From equations (1.105) and (3.73), we have

$$\langle p_i \rangle = -\frac{1}{2}\mathrm{Re}(v_j^* \sigma_{ij}). \tag{3.106}$$

From (3.2) and (3.21) and using the relation $\mathcal{K} = \mathcal{E} - 2\mu(1 - 1/n)$ (see (3.23)), we write the stress-strain relation as

$$\sigma_{ij} = \left(\mathcal{K} - \frac{2}{n}\mu\right)\epsilon_{kk}\delta_{ij} + 2\mu\epsilon_{ij} = \mathcal{E}\epsilon_{kk}\delta_{ij} + 2\mu(\epsilon_{ij} - \epsilon_{kk}\delta_{ij}). \tag{3.107}$$

The following expressions are obtained for the plane wave (3.25),

$$v_j^* = \omega\Phi_0^* k_j^* \exp[-\mathrm{i}(\omega t - \mathbf{k}^* \cdot \mathbf{x})] = \omega k_j^* \Phi^*, \tag{3.108}$$

$$\epsilon_{kk} = -k^2\Phi \tag{3.109}$$

and

$$\epsilon_{ij} = -k_i k_j \Phi. \tag{3.110}$$

Substituting these expressions into equations (3.106) and (3.107) yields

$$\langle p_i \rangle = \frac{1}{2}\omega|\Phi_0|^2 \exp(-2\boldsymbol{\alpha} \cdot \mathbf{x})\mathrm{Re}[\mathcal{E}k_j^* k^2 \delta_{ij} + 2\mu k_j^*(k_i k_j - k^2\delta_{ij})], \tag{3.111}$$

or, using (3.24), we have

$$\langle p_i \rangle = \frac{1}{2}\omega|\Phi_0|^2 \exp(-2\boldsymbol{\alpha}\cdot\mathbf{x})\mathrm{Re}[\rho\omega^2 k_j^*\delta_{ij} + 2\mu k_j^*(k_ik_j - k^2\delta_{ij})]. \tag{3.112}$$

We can now write

$$\begin{aligned} k_j^*(k_ik_j - k^2\delta_{ij}) &= \mathbf{k}\cdot\mathbf{k}^* k_i - \mathbf{k}\cdot\mathbf{k}\ k_i^* \\ &= (\boldsymbol{\kappa}\cdot\boldsymbol{\kappa} + \boldsymbol{\alpha}\cdot\boldsymbol{\alpha})k_i - (\boldsymbol{\kappa}\cdot\boldsymbol{\kappa} - \boldsymbol{\alpha}\cdot\boldsymbol{\alpha} - 2\mathrm{i}\boldsymbol{\alpha}\cdot\boldsymbol{\kappa})k_i^* \\ &= \boldsymbol{\kappa}\cdot\boldsymbol{\kappa}(k_i - k_i^*) + \boldsymbol{\alpha}\cdot\boldsymbol{\alpha}(k_i + k_i^*) + 2\mathrm{i}\boldsymbol{\alpha}\cdot\boldsymbol{\kappa}\ k_i^* \\ &= 2\mathrm{i}\boldsymbol{\kappa}\cdot\boldsymbol{\kappa}\ \mathrm{Im}(k_i) + 2\boldsymbol{\alpha}\cdot\boldsymbol{\alpha}\ \mathrm{Re}(k_i) + 2\mathrm{i}\boldsymbol{\alpha}\cdot\boldsymbol{\kappa}\ k_i^* \end{aligned} \tag{3.113}$$

or, in vector form

$$\begin{aligned} \text{vector} &= -2\mathrm{i}(\boldsymbol{\kappa}\cdot\boldsymbol{\kappa})\boldsymbol{\alpha} + 2(\boldsymbol{\alpha}\cdot\boldsymbol{\alpha})\boldsymbol{\kappa} + 2\mathrm{i}(\boldsymbol{\alpha}\cdot\boldsymbol{\kappa})(\boldsymbol{\kappa} + \mathrm{i}\boldsymbol{\alpha}) \\ &= 2\boldsymbol{\kappa}[\boldsymbol{\alpha}\cdot(\mathrm{i}\boldsymbol{\kappa} + \boldsymbol{\alpha})] - 2\boldsymbol{\alpha}[\boldsymbol{\kappa}\cdot(\mathrm{i}\boldsymbol{\kappa} + \boldsymbol{\alpha})] \\ &= 2(\mathrm{i}\boldsymbol{\kappa} + \boldsymbol{\alpha})\times(\boldsymbol{\kappa}\times\boldsymbol{\alpha}) = -2(\boldsymbol{\kappa}\times\boldsymbol{\alpha})\times(\mathrm{i}\boldsymbol{\kappa} + \boldsymbol{\alpha}), \end{aligned} \tag{3.114}$$

where we have used the property $\mathbf{a}\times(\mathbf{b}\times\mathbf{c}) = (\mathbf{a}\cdot\mathbf{c})\mathbf{b} - (\mathbf{a}\cdot\mathbf{b})\mathbf{c}$ (Brand, 1957, p. 31).

Substituting equation (3.114) into equation (3.112) and taking the real part, we obtain the final form of the time-averaged power flow, namely,

$$\langle \mathbf{p} \rangle = \frac{1}{2}\omega|\Phi_0|^2 \exp(-2\boldsymbol{\alpha}\cdot\mathbf{x})[\rho\omega^2\boldsymbol{\kappa} + 4(\boldsymbol{\kappa}\times\boldsymbol{\alpha})\times(\mu_I\boldsymbol{\kappa} - \mu_R\boldsymbol{\alpha})]. \tag{3.115}$$

We can infer that the energy propagates in the plane of $\boldsymbol{\kappa}$ and $\boldsymbol{\alpha}$, but not in the direction perpendicular to the wave surface, as is the case with elastic materials and homogeneous viscoelastic waves, for which $\boldsymbol{\kappa}\times\boldsymbol{\alpha} = 0$.

Let us perform the scalar product of the time-averaged energy flow $\langle \mathbf{p} \rangle$ with the attenuation vector $\boldsymbol{\alpha}$. The second term contains the scalar triple product $[(\boldsymbol{\kappa}\times\boldsymbol{\alpha})\times(\mathrm{i}\boldsymbol{\kappa} + \boldsymbol{\alpha})]\cdot\boldsymbol{\alpha}$ (see equation (3.114)). Using the property of the triple product $(\mathbf{a}\times\mathbf{b})\cdot\mathbf{c} = (\mathbf{b}\times\mathbf{c})\cdot\mathbf{a}$ (Brand, 1957, p. 33), we have

$$[(\boldsymbol{\kappa}\times\boldsymbol{\alpha})\times(\mathrm{i}\boldsymbol{\kappa} + \boldsymbol{\alpha})]\cdot\boldsymbol{\alpha} = [(\mathrm{i}\boldsymbol{\kappa} + \boldsymbol{\alpha})\times\boldsymbol{\alpha}]\cdot(\boldsymbol{\kappa}\times\boldsymbol{\alpha}) = \mathrm{i}|\boldsymbol{\kappa}\times\boldsymbol{\alpha}|^2. \tag{3.116}$$

Using this equation, we obtain

$$\langle \mathbf{p} \rangle \cdot \boldsymbol{\alpha} = \frac{1}{2}\langle \dot{D} \rangle, \tag{3.117}$$

or

$$\langle \dot{D} \rangle = 2\langle \mathbf{p} \rangle \cdot \boldsymbol{\alpha}, \tag{3.118}$$

where $\langle \dot{D} \rangle$ is the time-averaged rate of dissipated energy (3.99). Moreover, since

$$2\langle \mathbf{p} \rangle \cdot \boldsymbol{\alpha} = \langle \dot{D} \rangle = -\langle \mathrm{div}\ \mathbf{p} \rangle, \tag{3.119}$$

we can infer from equations (3.75) and (3.104) that the mean value of the rate of total energy density vanishes

$$\langle \partial_t E \rangle = 0. \tag{3.120}$$

On the other hand, if we calculate the scalar product between the time-averaged energy-flow vector $\langle \mathbf{p} \rangle$ and the wavenumber vector $\boldsymbol{\kappa}$, we obtain $|\boldsymbol{\kappa}\times\boldsymbol{\alpha}|^2$ for the corresponding triple product. Using this fact, we obtain the following relation

$$\omega\langle E \rangle = \langle \mathbf{p} \rangle \cdot \boldsymbol{\kappa}. \tag{3.121}$$

As in the 1-D case (equation (2.114)) and the lossless anisotropic case (equation (1.113)), we define the energy-velocity vector as the ratio of the time-averaged energy-flow vector to the time-averaged energy density,

$$\mathbf{v}_e = \frac{\langle \mathbf{p} \rangle}{\langle E \rangle}. \tag{3.122}$$

Combining (3.121) and (3.122), we obtain the relation

$$\hat{\boldsymbol{\kappa}} \cdot \mathbf{v}_e = v_p, \qquad (\mathbf{s}_R \cdot \mathbf{v}_e = 1), \tag{3.123}$$

where v_p and $\mathbf{s}_R$ are the phase velocity and slowness vector introduced in (3.37). This can be interpreted as the lines of constant phase traveling with velocity v_e in the direction of $\langle \mathbf{p} \rangle$. This property is satisfied by plane waves propagating in an anisotropic elastic medium (see equation (1.114)). Here, the relation also holds for inhomogeneous viscoelastic plane waves. For homogeneous waves, $\gamma = 0$, $\boldsymbol{\kappa} \times \boldsymbol{\alpha} = 0$, equations (3.104) and (3.115) become

$$\langle E \rangle = \frac{1}{2} |\Phi_0|^2 \exp(-2\boldsymbol{\alpha} \cdot \mathbf{x}) \rho \omega^2 |\boldsymbol{\kappa}|^2 \tag{3.124}$$

and

$$\langle \mathbf{p} \rangle = \frac{1}{2} \omega |\Phi_0|^2 \exp(-2\boldsymbol{\alpha} \cdot \mathbf{x}) \rho \omega^2 \boldsymbol{\kappa}, \tag{3.125}$$

and we have $\mathbf{v}_e = \mathbf{v}_p$.

As in the 1-D case (equation (2.119)), we define the quality factor as

$$Q = \frac{2\langle V \rangle}{\langle D \rangle}, \tag{3.126}$$

where

$$\langle D \rangle \equiv \omega^{-1} \langle \dot{D} \rangle \tag{3.127}$$

is the time-averaged dissipated-energy density. Substituting the time-averaged strain-energy density (3.97) and the time-averaged rate of dissipated-energy density (3.99), and using equations (3.18) and (3.33), we obtain

$$Q = \frac{\kappa^2 - \alpha^2}{2\kappa\alpha} = -\frac{\mathrm{Re}(k^2)}{\mathrm{Im}(k^2)} = \frac{\mathrm{Re}(v_c^2)}{\mathrm{Im}(v_c^2)}, \tag{3.128}$$

where we assumed homogeneous waves ($\gamma = 0$). As in the 1-D case, we obtain the relation

$$\alpha = \frac{\pi f}{Q v_p} \tag{3.129}$$

for $Q \gg 1$ and homogeneous plane waves. On the other hand, definition (2.124) and equations (3.118), (3.122) and (3.127) imply

$$\mathcal{Q} = \frac{\langle E \rangle}{\langle D \rangle} = \frac{\omega \langle E \rangle}{\langle \dot{D} \rangle} = 2 \left(\frac{\omega \langle E \rangle}{\langle \mathbf{p} \rangle \cdot \boldsymbol{\alpha}} \right) = \frac{\omega}{2\mathbf{v}_e \cdot \boldsymbol{\alpha}}. \tag{3.130}$$

For homogeneous waves, this equation implies the relation

$$\alpha = \frac{\pi f}{\mathcal{Q} v_p}, \tag{3.131}$$

which holds without requiring the condition $Q \gg 1$.

3.4.2 S waves

The results for the type-I S wave have the same form as those for the P wave, while the results for the type-II S wave are similar, but differ by a factor of 2 in the inhomogeneous term. We have

$$\begin{aligned}
\langle \mathbf{p} \rangle &= \tfrac{1}{2}\omega|\Xi_0|^2 \exp(-2\boldsymbol{\alpha}\cdot\mathbf{x})[\rho\omega^2\boldsymbol{\kappa} + a(\boldsymbol{\kappa}\times\boldsymbol{\alpha})\times(\mu_I\boldsymbol{\kappa} - \mu_R\boldsymbol{\alpha})],\\
\langle T \rangle &= \tfrac{1}{4}\rho\omega^2|\Xi_0|^2 \exp(-2\boldsymbol{\alpha}\cdot\mathbf{x})(|\boldsymbol{\kappa}|^2 + |\boldsymbol{\alpha}|^2),\\
\langle V \rangle &= \tfrac{1}{4}|\Xi_0|^2 \exp(-2\boldsymbol{\alpha}\cdot\mathbf{x})[\rho\omega^2(|\boldsymbol{\kappa}|^2 - |\boldsymbol{\alpha}|^2) + 2a\mu_R|\boldsymbol{\kappa}\times\boldsymbol{\alpha}|^2],\\
\langle E \rangle &= \tfrac{1}{2}|\Xi_0|^2 \exp(-2\boldsymbol{\alpha}\cdot\mathbf{x})[\rho\omega^2|\boldsymbol{\kappa}|^2 + a\mu_R|\boldsymbol{\kappa}\times\boldsymbol{\alpha}|^2],\\
\langle \dot{D} \rangle &= \omega|\Xi_0|^2 \exp(-2\boldsymbol{\alpha}\cdot\mathbf{x})[\rho\omega^2(\boldsymbol{\kappa}\cdot\boldsymbol{\alpha}) + a\mu_I|\boldsymbol{\kappa}\times\boldsymbol{\alpha}|^2],
\end{aligned} \tag{3.132}$$

where $\Xi_0 = \Phi_0$ and $a = 4$ for P waves, $\Xi_0 = \Theta_0$ and $a = 4$ for type-I S waves, and $\Xi_0 = \Gamma_0/(\mathbf{k}\cdot\mathbf{k}^*)$ and $a = 2$ for type-II S waves (see equations (3.25), (3.57) (3.59)). Some details of the preceding equations can be found in Buchen (1971a) and Krebes (1983a), and in Caviglia and Morro (1992, pp. 57-60), where an additional correction term is added to the time-averaged energy-flow vector of the type-I S wave. Moreover, relations (3.120), (3.123) and (3.118) are valid in general, as are the expressions for the energy velocity and quality factor (3.122) and (3.128), respectively. The extension to isotropic poro-viscoelastic media is given by Rasolofosaon (1991).

3.5 Boundary conditions and Snell's law

A picture illustrating the reflection-transmission phenomenon is shown in Figure 3.5, where the vectors $\boldsymbol{\kappa}$, $\boldsymbol{\alpha}$ and $\hat{\mathbf{n}}$ need not be coplanar.

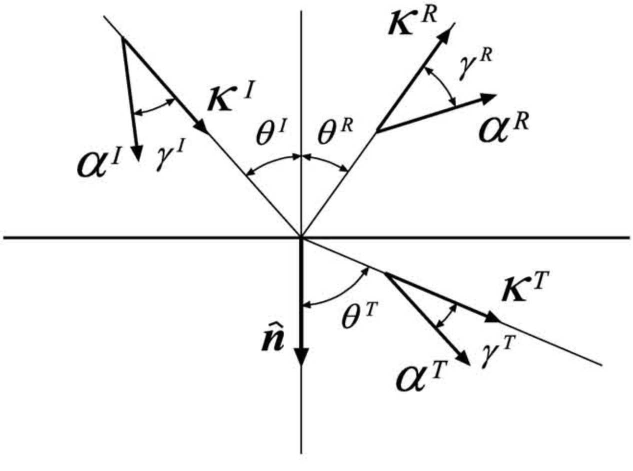

Figure 3.5: The reflection-transmission problem in viscoelastic media.

Depending on the nature of the incident waves, four or two waves are generated at the interface, corresponding to the P-SV (P-(S-I)) and SH/SH ((S-II)-(S-II)) scattering problems. If the two media are in welded contact, the boundary conditions are the continuity of the displacements (or particle velocities) and normal stresses across the interface, that is continuity of

$$u_i \quad \text{and} \quad \sigma_{ij} n_j \tag{3.133}$$

(Auld, 1990a, p. 124). This implies that the complex phase $\mathbf{k} \cdot \mathbf{x}$ at any point of the interface is the same for all the waves involved in the process, that is

$$\mathbf{k}^I \cdot \mathbf{x} = \mathbf{k}^R \cdot \mathbf{x} = \mathbf{k}^T \cdot \mathbf{x}, \qquad \mathbf{x} \cdot \hat{\mathbf{n}} = 0, \tag{3.134}$$

or

$$\mathbf{k}^I \times \hat{\mathbf{n}} = \mathbf{k}^R \times \hat{\mathbf{n}} = \mathbf{k}^T \times \hat{\mathbf{n}}. \tag{3.135}$$

In terms of the complex wavevector $\mathbf{k}$ and slowness vector $\mathbf{s} = \mathbf{k}/\omega$, and identifying the interface with the plane $z = 0$, we have

$$k_1^I = k_1^R = k_1^T \quad \text{and} \quad k_2^I = k_2^R = k_2^T, \tag{3.136}$$

$$s_1^I = s_1^R = s_1^T \quad \text{and} \quad s_2^I = s_2^R = s_2^T. \tag{3.137}$$

This general form of Snell's law implies the continuity at the interface of the tangential component of the real and imaginary parts of the complex wavevector (or complex-slowness vector) and, therefore, the continuity of the tangential components of $\boldsymbol{\kappa}$ and $\boldsymbol{\alpha}$. This condition can be written as

$$\begin{aligned} &\kappa^I \sin\theta^I = \kappa^R \sin\theta^R = \kappa^T \sin\theta^T \\ &\alpha^I \sin(\theta^I - \gamma^I) = \alpha^R \sin(\theta^R - \gamma^R) = \alpha^T \sin(\theta^T - \gamma^T). \end{aligned} \tag{3.138}$$

It is not evident from this equation that the reflection angle is equal to the incidence angle for waves of the same type. Because k^2 is a material property independent of the inhomogeneity angle (see equation (3.24)), the relation

$$k_3^2 = k^2 - (k_1^2 + k_2^2) \tag{3.139}$$

and equation (3.136) imply $k_3^{I^2} = k_3^{R^2}$. Since the z-components of the incident and reflected waves should have opposite signs, we have

$$k_3^R = -k_3^R. \tag{3.140}$$

This relation and equation (3.136) imply $\kappa^I = \kappa^R$ and $\alpha^I = \alpha^R$, and from (3.138)

$$\theta^R = \theta^I \quad \text{and} \quad \gamma^R = \gamma^I. \tag{3.141}$$

Therefore, the reflected wave is homogeneous only if the incident wave is homogeneous. More consequences from the viscoelastic nature of Snell's law are discussed in Section 3.8, where we solve the problem of reflection and transmission of SH waves[1].

[1]Note that to obtain Snell's law we have not used the assumption of isotropy. Thus, equations (3.138) are also valid for anisotropic anelastic media.

3.6 The correspondence principle

The correspondence principle allows us to obtain viscoelastic solutions from the corresponding elastic (lossless) solutions. The stress-strain relation (3.2) can be rewritten as

$$\sigma_{ij} = \psi_{\mathcal{K}} * \partial_t \epsilon_{kk} \delta_{ij} + 2\psi_\mu * \partial_t d_{ij}, \tag{3.142}$$

where d_{ij} is defined in equation (3.6).

Note that the Fourier transform of the stress-strain relations (3.142) is

$$\sigma_{ij}(\omega) = \mathcal{K}(\omega)\epsilon_{kk}(\omega)\delta_{ij} + 2\mu(\omega)d_{ij}(\omega), \tag{3.143}$$

where

$$\mathcal{K}(\omega) = \mathcal{F}[\partial_t \psi_{\mathcal{K}}(t)] \quad \text{and} \quad \mu(\omega) = \mathcal{F}[\partial_t \psi_\mu(t)] \tag{3.144}$$

are the corresponding complex moduli. The form (3.143) is similar to the stress-strain relation of linear elasticity theory, except that the moduli are complex and frequency dependent. Note also that Euler's differential equations (1.23) are the same for lossy and lossless media. Therefore, if the elastic solution is available, the viscoelastic solution is obtained by replacing the elastic moduli with the corresponding viscoelastic moduli. This is known as the correspondence principle[2]. We show specific examples of this principle in Section 3.10. Extensions of the correspondence principle are given in Golden and Graham (1988, p. 68).

3.7 Rayleigh waves

The importance of Rayleigh waves can be noted in several fields, from earthquake seismology to material science (Parker and Maugin, 1988; Chadwick, 1989). The first theoretical investigations carried out by Lord Rayleigh (1885) in isotropic elastic media showed that these waves are confined to the surface and, therefore, they do not scatter in depth as do seismic body waves.

Hardtwig (1943) was the first to study viscoelastic Rayleigh waves, though he erroneously restricts their existence to a particular choice of the complex Lamé parameters. Scholte (1947) rectifies this mistake and verifies that the waves always exist in viscoelastic solids. He also predicts the existence of a second surface wave, mainly periodic with depth, whose exponential damping is due to anelasticity and not to the Rayleigh character – referred to later as v.e. mode. Caloi (1948) and Horton (1953) analyze the anelastic characteristics and displacements of the waves considering a Voigt-type dissipation mechanism with small viscous damping, and a Poisson solid. Borcherdt (1973) analyzes the particle motion at the free surface and concludes that the differences between elastic and viscoelastic Rayleigh waves arise from differences in their components: the usual inhomogeneous plane waves in the elastic case, and viscoelastic inhomogeneous plane waves in the anelastic case, which allow any angle between the propagation and attenuation vectors.

[2] Although the principle has been illustrated for isotropic media, its extension to the anisotropic case can be obtained by taking the Fourier transform of the stress-strain relation (2.22), which leads to equation (4.4).

A complete analysis is carried out by Currie, Hayes and O'Leary (1977), Currie and O'Leary (1978) and Currie (1979). They show that for viscoelastic Rayleigh waves: (i) more than one wave is possible, (ii) the particle motion may be either direct or retrograde at the surface, (iii) the motion may change sense at many or no levels with depth, (iv) the wave energy velocity may be greater than the body waves energy velocities. They refer to the wave that corresponds to the usual elastic surface wave as quasi-elastic (q.e.), and to the wave that only exists in the viscoelastic medium as viscoelastic (v.e.). This mode is possible only for certain combinations of the complex Lamé constants and for a given range of frequencies. Using the method of generalized rays, Borejko and Ziegler (1988) study the characteristics of the v.e. surface waves for the Maxwell and Kelvin-Voigt solids.

3.7.1 Dispersion relation

Since the medium is isotropic, we assume without loss of generality that the wave propagation is in the (x, z)-plane with $z = 0$ being the free surface. Let a plane-wave solution to equation (1.23) be of the form

$$\mathbf{u} = \mathbf{U} \exp[\mathrm{i}(\omega t - \mathbf{k} \cdot \mathbf{x})]. \tag{3.145}$$

For convenience, let m =1 denote the compressional wave and $m = 2$ the shear wave. We rewrite the dispersion relations (3.24) as

$$k^{(m)2} = \frac{\omega^2}{v_m^2}, \quad v_1^2 = \frac{\mathcal{E}}{\rho}, \quad v_2^2 = \frac{\mu}{\rho}, \tag{3.146}$$

where $\mathcal{E}(\omega) = \lambda(\omega) + 2\mu(\omega)$.

A general solution is given by the superposition of the compressional and shear modes,

$$\mathbf{u} = \mathbf{U}^{(m)} \exp[\mathrm{i}(\omega t - \mathbf{k}^{(m)} \cdot \mathbf{x})], \tag{3.147}$$

where

$$\mathbf{U}^{(1)} = U_0 \mathbf{k}^{(1)}, \qquad \mathbf{U}^{(2)} \cdot \mathbf{k}^{(2)} = 0. \tag{3.148}$$

At the free surface ($z = 0$), the boundary conditions are

$$\sigma_{33} = \lambda \partial_1 u_1 + (\lambda + 2\mu)\partial_3 u_3 = 0, \quad \text{and} \quad \sigma_{13} = \mu(\partial_1 u_3 + \partial_3 u_1) = 0. \tag{3.149}$$

These boundary conditions imply that the horizontal wavenumber is the same for each mode,

$$k_1^{(1)} = k_1^{(2)} \equiv k_1 = \kappa_1 - \mathrm{i}\alpha_1. \tag{3.150}$$

From equations (3.147) and (3.150), the displacement components are

$$\begin{aligned} u_1 &= F(z) \exp[\mathrm{i}(\omega t - k_1 x)], \qquad F(z) = U_1^{(m)} \exp(-\mathrm{i}k_3^{(m)} z), \\ u_3 &= G(z) \exp[\mathrm{i}(\omega t - k_1 x)], \qquad G(z) = U_3^{(m)} \exp(-\mathrm{i}k_3^{(m)} z), \end{aligned} \tag{3.151}$$

where the vertical wavenumbers are

$$k_3^{(m)} = \kappa_3^{(m)} - \mathrm{i}\alpha_3^{(m)}. \tag{3.152}$$

From equations (3.146), (3.148) and (3.150),

$$k_3^{(m)2} = \frac{\omega^2}{v_m^2} - k_1^2 = \omega^2 \left(\frac{1}{v_m^2} - \frac{1}{v_c^2} \right), \tag{3.153}$$

and

$$\frac{U_3^{(1)}}{U_1^{(1)}} = \frac{k_3^{(1)}}{k_1} = \sqrt{\frac{v_c^2}{v_1^2} - 1}, \quad \frac{U_3^{(2)}}{U_1^{(2)}} = -\frac{k_1}{k_3(2)} = -\left(\frac{v_c}{v_2^2} - 1 \right)^{-1/2}, \tag{3.154}$$

where

$$v_c = \frac{\omega}{k_1} \tag{3.155}$$

is the Rayleigh-wave complex velocity. The boundary conditions (3.149) and equations (3.154) imply

$$\frac{U_1^{(2)}}{U_1^{(1)}} = \frac{v_c^2}{2v_2^2} - 1 \equiv A \tag{3.156}$$

and

$$A^2 + \frac{k_3^{(1)} k_3^{(2)}}{k_1^2} = 0. \tag{3.157}$$

The squaring of (3.157) and reordering of terms gives a cubic equation for the complex velocity,

$$q^3 - 8q^2 + \left(24 - 16\frac{v_2^2}{v_1^2} \right) q - 16 \left(1 - \frac{v_2^2}{v_1^2} \right) = 0, \quad q = \frac{v_c^2}{v_2^2}, \tag{3.158}$$

which could, alternatively, be obtained by using the correspondence principle (see Section 3.6) and the elastic Rayleigh-wave dispersion relation. The dispersion relation (3.158), together with equation (3.157), may determine one or more wave solutions. The solution of the q.e. surface wave is always possible, since it is the equivalent of the elastic Rayleigh wave. The other surface waves, called v.e. modes, are possible depending on the frequency and the material properties (Currie, 1979).

3.7.2 Displacement field

The amplitude coefficients may be referred to $U_1^{(1)} = 1$ without loss of generality. Thus, from equations (3.154) and (3.156),

$$U_1^{(1)} = 1, \quad U_1^{(2)} = A, \quad U_3^{(1)} = \frac{k_3^{(1)}}{k_1}, \quad U_3^{(2)} = \frac{k_3^{(1)}}{k_1 A}. \tag{3.159}$$

From these equations, the displacements (3.151) become

$$\begin{aligned} u_1 &= [\exp(-\mathrm{i}k_3^{(1)} z) + A \exp(-\mathrm{i}k_3^{(2)} z)] \exp[\mathrm{i}(\omega t - k_1 x)], \\ u_3 &= (k_3^{(1)}/k_1) \left[\exp(-\mathrm{i}k_3^{(1)} z) + A^{-1} \exp(-\mathrm{i}k_3^{(2)} z) \right] \exp[\mathrm{i}(\omega t - k_1 x)]. \end{aligned} \tag{3.160}$$

These displacements are a combination of compressional and shear modes, with the phase factors

$$\exp\{\mathrm{i}[\omega t - (\kappa_1 x + \kappa_3^{(m)} z)]\} \exp[-(\alpha_1 x + \alpha_3^{(m)} z)], \quad m = 1, 2, \tag{3.161}$$

given by virtue of equations (3.150) and (3.152). It is clear, from the last equation, that to have attenuating waves, a physical solution of equation (3.158) must satisfy the following conditions:

$$\alpha_1 > 0, \quad \alpha_3^{(m)} > 0, \quad \kappa_1 > 0. \tag{3.162}$$

The last condition imposes wave propagation along the positive x-direction. In terms of the complex velocities, these conditions read

$$-\omega \mathrm{Im}\left(\frac{1}{v_c}\right) > 0, \quad -\mathrm{Im}\left(\sqrt{\frac{1}{v_m^2} - \frac{1}{v_c^2}}\right) > 0, \quad \omega \mathrm{Re}\left(\frac{1}{v_c}\right) > 0. \tag{3.163}$$

Also, equation (3.157) must be satisfied in order to avoid spurious roots.

3.7.3 Phase velocity and attenuation factor

The phase velocity in the x-direction is defined as the frequency divided by the x-component of the real wavenumber κ_1,

$$v_p \equiv \frac{\omega}{\kappa_1} = \frac{\omega}{\mathrm{Re}(k_1)} = \left[\mathrm{Re}\left(\frac{1}{v_c}\right)\right]^{-1}. \tag{3.164}$$

From equation (3.161), the phase velocities associated with each component wave mode are

$$\mathbf{v}_{pm} = \omega \left(\frac{\kappa_1 \hat{\mathbf{e}}_1 + \kappa_3^{(m)} \hat{\mathbf{e}}_3}{\kappa_1^2 + \kappa_3^{(m)2}}\right), \quad \text{and} \quad \mathbf{v}_{pm} = \left(\frac{\omega}{\kappa_1}\right) \hat{\mathbf{e}}_1, \quad \text{(lossless case)}. \tag{3.165}$$

In the elastic (lossless) case, there is only a single and physical solution to equation (3.158). Moreover, because the velocities are real and $v_c < v_2 < v_1$, $k_3^{(1)}$ and $k_3^{(2)}$ are purely imaginary and $\kappa_3^{(m)} = 0$. Hence, $v_{pm} = v_p$, and equation (3.161) reduces to

$$\exp[\mathrm{i}(\omega t - \kappa_1 x)] \exp(-\alpha_3^{(m)} z), \tag{3.166}$$

with $\kappa_1 = k_1$ and $\alpha_3^{(m)} = \mathrm{i} k_3^{(m)}$. In this case, the propagation vector points along the surface and the attenuation vector is normal to the surface. However, in a viscoelastic medium, according to equation $(3.165)_1$, these vectors are inclined with respect to those directions.

The attenuation factor in the x-direction is given by

$$\alpha = -\omega \ \mathrm{Im}\left(\frac{1}{v_c}\right) > 0. \tag{3.167}$$

Each wave mode has an attenuation vector given by

$$\alpha_1 \hat{\mathbf{e}}_1 + \alpha_3^{(m)} \hat{\mathbf{e}}_3, \quad \text{and} \quad \alpha_3^{(m)} \hat{\mathbf{e}}_3 \ \text{(lossless case)}. \tag{3.168}$$

Carcione (1992b) calculates the energy-balance equation and shows that, in contrast to elastic materials, the energy flow is not directed along the surface and the energy velocity is not equal to the phase velocity.

3.7.4 Special viscoelastic solids

Incompressible solid

Incompressibility implies $\lambda \rightarrow \infty$, or, equivalently, $v_1 \rightarrow \infty$. Hence, from equation (3.158), the dispersion relation becomes

$$q^3 - 8q^2 + 24q - 16 = 0. \tag{3.169}$$

The roots are $q_1 = 3.5437 + \mathrm{i}\ 2.2303$, $q_2 = 3.5437 - \mathrm{i}\ 2.2303$ and $q_3 = 0.9126$. As shown by Currie, Hayes and O'Leary (1977), two Rayleigh waves exist, the quasi-elastic mode, represented by q_3, and the viscoelastic mode, represented by q_1, which is admissible if $\mathrm{Im}(v_2^2)/\mathrm{Re}(v_2^2) > 0.159$, in order to fulfill conditions (3.162). In Currie, Hayes and O'Leary (1977), the viscoelastic root is given by q_2, since they use the opposite sign convention to compute the time-Fourier transform (see also Currie, 1979). Carcione (1992b) shows that at the surface, the energy velocity is equal to the phase velocity.

Poisson solid

A Poisson solid has $\lambda = \mu$, so that $v_1 = \sqrt{3}v_2$ and, therefore, equation (3.158) becomes

$$3q^3 - 24q^2 + 56q - 32 = 0. \tag{3.170}$$

This equation has three real roots: $q_1 = 4$, $q_2 = 2 + 2 \,/\, \sqrt{3}$, and $q_3 = 2 - 2 \,/\, \sqrt{3}$. The last root corresponds to the q.e. mode. The other two roots do not satisfy equation (3.157) and, therefore, there are no v.e. modes in a Poisson solid. As with the incompressible solid, the energy velocity is equal to the phase velocity at the surface.

Hardtwig solid

Hardtwig (1943) investigates the properties of a viscoelastic Rayleigh wave for which $\mathrm{Re}(\lambda)/\mathrm{Re}(\mu) = \mathrm{Im}(\lambda)/\mathrm{Im}(\mu)$. In this case, the coefficients of the dispersion relation (3.158) are real, ensuring at least one real root corresponding to the q.e. mode. This implies that the energy velocity coincides with the phase velocity at the surface (Carcione, 1992b). A Poisson medium is a particular type of Hardtwig solid.

3.7.5 Two Rayleigh waves

Carcione (1992b) studies a medium with $\rho = 2$ gr/cm^3, and complex Lamé constants

$$\lambda = (-1.15 - \mathrm{i}\ 0.197)\ \mathrm{GPa}, \qquad \mu = (4.91 + \mathrm{i}\ 0.508)\ \mathrm{GPa}$$

at a frequency of 20 Hz. The P-wave and S-wave velocities are 2089.11 m/s and 1573 m/s, respectively. Two roots satisfy equations (3.157) and (3.158): $q_1 = 0.711 - \mathrm{i}\ 0.0046$ corresponds to the q.e. mode, and $q_2 = 1.764 - \mathrm{i}\ 0.0156$ corresponds to the v.e. mode.

Figure 3.6 shows the absolute value of the horizontal and vertical displacements, $|u_1|$ and $|u_3|$, as a function of depth, for the q.e. Rayleigh wave (a) and the v.e. Rayleigh wave. Their phase velocities are 1326 m/s and 2089.27 m/s, respectively. The horizontal motion predominates in the v.e. Rayleigh wave and its phase velocity is very close to that of the P wave. For higher frequencies, this wave shows a strong oscillating behavior (Carcione, 1992b).

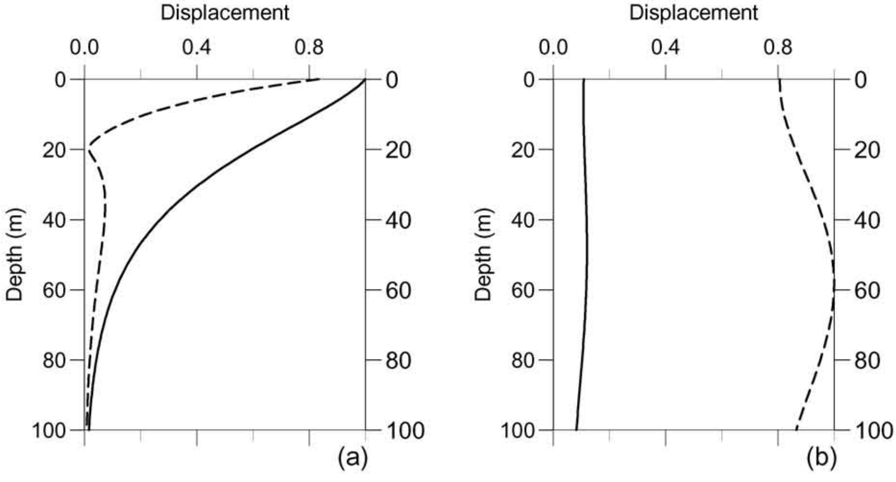

Figure 3.6: Absolute value of the horizontal and vertical displacements, $|u_1|$ (dashed line) and $|u_3|$ (solid line) versus depth, at a frequency of 20 Hz; (a) corresponds to the quasi-elastic Rayleigh wave, and (b) to the viscoelastic Rayleigh wave.

3.8 Reflection and transmission of cross-plane shear waves

The reflection-transmission problem in isotropic viscoelastic media is addressed by many researchers (for example, Cooper (1967), Buchen (1971b), Schoenberg (1971) and Stovas and Ursin (2001)). Borcherdt, Glassmoyer and Wennerberg (1986) present theoretical and experimental results and cite most of the relevant work carried out by R. Borcherdt on the subject. E. Krebes also contributes to the solution of the problem, mainly in connection with ray tracing in viscoelastic media (for example, Krebes, 1984; Krebes and Slawinski, 1991). A comprehensive review of the problem is given in Caviglia and Morro (1992).

In order to illustrate the main effects due to the presence of viscoelasticity, we analyze in some detail the reflection-transmission problem of SH waves at a plane interface, following Borcherdt (1977). The P-SV problem for transversely isotropic media (the symmetry axes are perpendicular to the interface) is analyzed in detail in Chapter 6.

The reflection and transmission coefficients for SH waves have the same form as the coefficients for lossless isotropic media, but they are not identical because the quantities involved are complex. Consequently, we may apply the correspondence principle (see Section 3.6) to the expressions found for perfect elastic media (equation (1.282)). We set $c_{46} = 0$, replace c_{44} and c_{66} by μ, and c'_{44} and c'_{66} by μ'. We obtain

$$R_{\rm SS} = \frac{Z^I - Z^T}{Z^I + Z^T}, \qquad T_{\rm SS} = \frac{2Z^I}{Z^I + Z^T}, \tag{3.171}$$

where

$$Z^I = \mu s_3^I, \quad s_3^I = \sqrt{\rho/\mu - s_1^2}, \tag{3.172}$$

and

$$Z^T = \pm\mu' \mathrm{pv}\sqrt{\rho'/\mu' - s_1^2}, \tag{3.173}$$

where pv denotes the principal value of the complex square root. (For the principal value, the argument of the square root lies between $-\pi/2$ and $+\pi/2$). As indicated by Krebes (1984), special care is needed when choosing the sign in equation (3.173), since a wrong choice may lead to discontinuities of the vertical wavenumber as a function of the incidence angle. Unlike the elastic case, the amplitude of the scattered waves can grow exponentially with distance from the interface (Richards, 1984). Thus, the condition of an exponentially decaying wave is not sufficient to obtain the reflection and transmission coefficients. Instead, the signs of the real and imaginary parts of s_3^T should be chosen to guarantee a smooth variation of s_3^T versus the incidence angle. Such an analysis is illustrated by Richards (1984).

Let us assume that the incident and transmitted waves are homogeneous. Then, $k = \kappa - \mathrm{i}\alpha$ (see equation (3.27)), $\gamma = 0$ and from Snell's law (3.138), we have that

$$\frac{k^{T2}}{k^2} = \frac{\sin^2\theta^I}{\sin^2\theta^T} \tag{3.174}$$

is a real quantity (we have omitted the superscript I in the wavenumber of the incident wave). This equation also implies the condition

$$\sin^2\theta^I \le \frac{k^{T2}}{k^2}. \tag{3.175}$$

Let us denote the quality factor of the homogeneous plane wave by Q_H, as defined in equation (3.32). As for P waves, the quality factor of homogeneous SH waves is given by equation (3.128). In this case, $Q_H = \mathrm{Re}(v_c^2)/\mathrm{Im}(v_c^2) = \mathrm{Re}(\mu)/\mathrm{Im}(\mu) = \mu_R/\mu_I$. We deduce from equation (3.31) that if $Q'_H = Q_H$, then k^{T^2}/k^2 is real and vice versa, and from $(3.24)_2$, $(3.37)_1$, and $(3.38)_1$, we note that

$$\frac{k^{T2}}{k^2} = \left(\frac{\rho'}{\rho}\right)\left(\frac{\mu_R}{\mu'_R}\right) = \frac{v_{pH}^2}{v_{pH}^{T\ 2}}. \tag{3.176}$$

Then, we may state a theorem attributed to Borcherdt (1977):

Theorem 1: If the incident SH wave is homogeneous and not normally incident, then the transmitted SH wave is homogeneous if and only if

$$Q'_H = Q_H, \quad \sin^2\theta^I \le \frac{k^{T2}}{k^2} = \left(\frac{\rho'}{\rho}\right)\left(\frac{\mu_R}{\mu'_R}\right) = \frac{v_{pH}^2}{v_{pH}^{T\ 2}}. \tag{3.177}$$

Let us analyze now the reflection coefficient when $Q'_H = Q_H$. We can write

$$\mu = \mu_R(1 + \mathrm{i}Q_H^{-1}) \equiv \mu_R W, \qquad \mu' = \mu'_R W. \tag{3.178}$$

Let us evaluate the numerator and denominator of R in equation (3.171) for precritical incidence angles ($\sin\theta^I \le v_{pH}/v_{pH}^T$). Using (3.172) and (3.173), we have

$$Z^I \pm Z^T = \mu\sqrt{\frac{\rho}{\mu} - s_1^2} \pm \mu'\sqrt{\frac{\rho'}{\mu'} - s_1^2}. \tag{3.179}$$

For a homogeneous wave $s_1 = \sin\theta^I/v_c$, where $v_c = \sqrt{\mu/\rho}$ is the complex shear-wave velocity. Using this relation and (3.178), equation (3.179) becomes

$$Z^I \pm Z^T = \sqrt{W}\left\{\sqrt{\rho\mu_R}\cos\theta^I \pm \sqrt{\rho'\mu'_R}\sqrt{1-\left(\frac{\rho\mu'_R}{\rho'\mu_R}\right)\sin^2\theta^I}\right\}. \tag{3.180}$$

Because W, which is the only complex quantity, appears as a multiplying factor in both the numerator and the denominator of R (see equation (3.171)), we obtain the expression of the elastic reflection coefficient (as if $Q_H^{-1} = {Q'_H}^{-1} = 0$). It can also be proved that for supercritical angles, the transmission coefficient is that of the lossless case. (See Krebes (1983b), or the reader can check these statements as an exercise). Note that there is no low-loss approximation, only the condition $Q'_H = Q_H$.

For lossless materials $Q_H = Q'_H = \infty$, and if $v_{pH}/v_{pH}^T < 1$, we have the well-known result that the transmitted wave is homogeneous if and only if $\sin\theta^I \leq v_{pH}/v_{pH}^T < 1$, with the equal sign corresponding to the critical angle (see equation (3.177)). Another consequence of Theorem 1 is that a normally incident homogeneous wave generates a homogeneous transmitted wave perpendicular to the interface. The most important consequence of Theorem 1 is that the transmitted wave will be, in general, inhomogeneous since in most cases $Q_H \neq Q'_H$. This implies that the velocity and the attenuation of the transmitted wave will be less than and greater than that of the corresponding homogeneous wave in the same medium. Moreover, the direction of energy flow will not coincide with the direction of phase propagation, and the velocity of the energy will not be equal to the phase velocity (see equation (3.123)).

The phase velocity of the transmitted wave is

$$v_p^{T2} = \frac{\omega^2}{\kappa^{T2}} = \frac{\omega^2}{\kappa_1^{T2} + \kappa_3^{T2}}, \tag{3.181}$$

where, from Snell's law

$$\kappa_1^T = \kappa_1, \tag{3.182}$$

$$\kappa_3^T = \pm\mathrm{Re}\left(\mathrm{pv}\sqrt{k^{T2} - k_1^{T2}}\right) = \pm\mathrm{Re}\left(\mathrm{pv}\sqrt{k^{T2} - k_1^2}\right). \tag{3.183}$$

For equation (3.183), we have assumed propagation in the x-direction, without loss of generality. Hence, unlike the lossless case, the phase velocity of the transmitted wave depends on the angles of incidence and on the inhomogeneity of the incident wave. From (3.138), the angle of refraction of the transmitted wave is

$$\frac{\sin^2\theta^T}{\sin^2\theta^I} = \frac{\kappa^2}{\kappa^{T2}} = \frac{{\kappa_1}^2 + {\kappa_3}^2}{{\kappa_1}^2 + \kappa_3^{T2}}, \tag{3.184}$$

which depends on the angles of incidence. Moreover, the dependence of the frequency of all these quantities through k^2 and k^{T^2} implies that an incident wave composed of different frequencies will transmit a fan of inhomogeneous waves at different angles. In the lossless case, each wave of different frequency is transmitted at the same angle.

Another important result, given below, is related to the existence of critical angles (Borcherdt, 1977).

Theorem 2: If the incidence medium is lossless and the transmission medium is anelastic, then there are no critical angles.

If θ^I is a critical angle, then $\theta^T = \pi/2$. Because the incidence medium is elastic, by Snell's law, the attenuation vector in the transmission medium is perpendicular to the interface and, hence, to the direction of propagation. However, since the transmission medium is anelastic, such a wave cannot exist (see condition (3.36) and equation (3.118)).

The analysis about the existence of critical angles and the energy flow and dissipation of the different waves is given in detail in Chapter 6, where the reflection-transmission problem of SH waves in the symmetry planes of monoclinic media is discussed. The main results are that critical angles in anelastic media exist only under very particular conditions, and that interference fluxes are not present in the lossless case (see Section 6.1.7). Some researchers define the critical angle as the angle of incidence for which the propagation angle of the transmitted wave is $\pi/2$, i.e., when the wavenumber vector $\boldsymbol{\kappa}$ is parallel to the interface (e.g., Borcherdt, 1977; Wennerberg, 1985, Caviglia, Morro and Pagani, 1989). This is not correct from a physical point of view. In Chapter 6, we adopt the criterion that the Umov-Poynting vector or energy-flow direction is parallel to the interface, which is the criterion used in anisotropic media. The two definitions coincide only in particular cases, because, in general, the phase-velocity and energy-velocity directions do not coincide. Theorem 2 is still valid when using the second criterion since the attenuation and Umov-Poynting vectors can never be perpendicular in an anelastic medium (see equation (3.118)).

3.9 Memory variables and equation of motion

The memory-variable approach introduced in Section 2.7 is essential to avoid numerical calculations of time convolutions when modeling wave propagation in the time domain. With this approach, we obtain a complete differential formulation. The relaxation functions in the stress-strain relation (3.142) for isotropic media have the form (2.198). We set

$$\psi_{\mathcal{K}}(t) = \mathcal{K}_\infty \left[1 - \frac{1}{L_1} \sum_{l=1}^{L_1} \left(1 - \frac{\tau_{\epsilon l}^{(1)}}{\tau_{\sigma l}^{(1)}}\right) \exp(-t/\tau_{\sigma l}^{(1)})\right] H(t), \tag{3.185}$$

$$\psi_{\mu}(t) = \mu_\infty \left[1 - \frac{1}{L_2} \sum_{l=1}^{L_2} \left(1 - \frac{\tau_{\epsilon l}^{(2)}}{\tau_{\sigma l}^{(2)}}\right) \exp(-t/\tau_{\sigma l}^{(2)})\right] H(t), \tag{3.186}$$

where $\tau_{\epsilon l}^{(\nu)}$ and $\tau_{\sigma l}^{(\nu)}$ are relaxation times corresponding to dilatational ($\nu = 1$) and shear ($\nu = 2$) attenuation mechanisms. They satisfy the condition (2.169), $\tau_{\epsilon l}^{(\nu)} \geq \tau_{\sigma l}^{(\nu)}$, with the equal sign corresponding to the elastic case.

In terms of the Boltzmann operation (2.6), equation (3.142) reads

$$\sigma_{ij} = \psi_{\mathcal{K}} \odot \epsilon_{kk}\delta_{ij} + 2\psi_\mu \odot d_{ij}, \tag{3.187}$$

or,

$$\sigma_{ij} = \mathcal{K}_U \left(\epsilon_{kk} + \sum_{l=1}^{L_1} e_l^{(1)}\right) \delta_{ij} + 2\mu_U \left(d_{ij} + \sum_{l=1}^{L_2} e_{ijl}^{(2)}\right), \tag{3.188}$$

where

$$\mathcal{K}_U = \frac{\mathcal{K}_\infty}{L_1} \sum_{l=1}^{L_1} \frac{\tau_{\epsilon l}^{(1)}}{\tau_{\sigma l}^{(1)}}, \qquad \mu_U = \frac{\mu_\infty}{L_2} \sum_{l=1}^{L_2} \frac{\tau_{\epsilon l}^{(2)}}{\tau_{\sigma l}^{(2)}}, \tag{3.189}$$

and

$$e_l^{(1)} = \varphi_{1l} * \epsilon_{kk}, \quad l = 1, \ldots, L_1 \tag{3.190}$$

and

$$e_{ijl}^{(2)} = \varphi_{2l} * d_{ij}, \quad l = 1, \ldots, L_2 \tag{3.191}$$

are sets of memory variables for dilatation and shear mechanisms, with

$$\breve{\varphi}_{\nu l} = \frac{1}{\tau_{\sigma l}^{(\nu)}} \left(\sum_{l=1}^{L_\nu} \frac{\tau_{\epsilon l}^{(\nu)}}{\tau_{\sigma l}^{(\nu)}} \right)^{-1} \left(1 - \frac{\tau_{\epsilon l}^{(\nu)}}{\tau_{\sigma l}^{(\nu)}} \right) \exp(-t/\tau_{\sigma l}^{(\nu)}). \tag{3.192}$$

As in the 1-D case (see equation (2.292)), the memory variables satisfy

$$\dot{e}_l^{(1)} = \varphi_{1l}(0)\epsilon_{kk} - \frac{e_l^{(1)}}{\tau_{\sigma l}^{(1)}}, \qquad \dot{e}_{ijl}^{(2)} = \varphi_{2l}(0) d_{ij} - \frac{e_{ijl}^{(2)}}{\tau_{\sigma l}^{(2)}}. \tag{3.193}$$

For $n = 2$ and say, the (x, z)-plane, we have three independent sets of memory variables. In fact, since $d_{11} = -d_{33} = (\epsilon_{11} - \epsilon_{33})/2$, then $e_{11l}^{(2)} = \varphi_{2l} * d_{11} = -\varphi_{2l} * d_{33}$. The other two sets are $e_l^{(1)} = \varphi_{1l} * \epsilon_{kk}$ and $e_{13l}^{(2)} = \varphi_{2l} * \epsilon_{13}$. In 3-D space ($n = 3$), there are six sets of memory variables, since $d_{11} + d_{22} + d_{33} = 0$ implies $e_{11l}^{(2)} + e_{22l}^{(2)} + e_{33l}^{(2)} = 0$, and two of these sets are independent. The other four sets are $e_l^{(1)} = \varphi_{1l} * \epsilon_{kk}$, $e_{23l}^{(2)} = \varphi_{2l} * \epsilon_{23}$, $e_{13l}^{(2)} = \varphi_{2l} * \epsilon_{13}$ and $e_{12l}^{(2)} = \varphi_{2l} * \epsilon_{12}$.

The equation of motion in 3-D space is obtained by substituting the stress-strain relation (3.188) into Euler's differential equations (1.23),

$$\begin{aligned} \partial_{tt}^2 u_1 &= \rho^{-1} \left(\partial_1 \sigma_{11} + \partial_2 \sigma_{12} + \partial_3 \sigma_{13} + f_1 \right) \\ \partial_{tt}^2 u_2 &= \rho^{-1} \left(\partial_1 \sigma_{12} + \partial_2 \sigma_{22} + \partial_3 \sigma_{23} + f_2 \right) \\ \partial_{tt}^2 u_3 &= \rho^{-1} \left(\partial_1 \sigma_{13} + \partial_2 \sigma_{23} + \partial_3 \sigma_{33} + f_3 \right), \end{aligned} \tag{3.194}$$

and making use of the strain-displacement relations (1.2)

$$\epsilon_{ij} = \frac{1}{2} (\partial_i u_j + \partial_j u_i). \tag{3.195}$$

In 2-D space and in the (x, z)-plane, all the derivatives ∂_2 vanish, u_2 is constant, and we should consider the first and third equations in (3.194). Applications of this modeling algorithm to compute the seismic response of reservoir models can be found in Kang and McMechan (1993), where Q effects are shown to be significant in both surface and offset vertical seismic profile data.

Assuming $L_1 = L_2$ and grouping the memory variables in the equation for each displacement component, the number of memory variables can be reduced to 2 in 2-D space and 3 in 3-D space (Xu and McMechan, 1995). Additional memory-storage savings can be achieved by setting $\tau_{\sigma l}^{(1)} = \tau_{\sigma l}^{(2)}$ (Emmerich and Korn, 1987). To further reduce storage, only a single relaxation time can be assigned to each grid point if a direct method is used to solve the viscoacoustic equation of motion (Day, 1998). A suitable spatial distribution of these relaxation times simulates the effects of the full relaxation spectrum.

3.10 Analytical solutions

Analytical solutions are useful to study the physics of wave propagation and test numerical modeling algorithms. They are essential in anelastic wave simulation to distinguish between numerical dispersion – due to the time and space discretization – and physical velocity dispersion. As stated in Section 3.6, if the elastic solution is available in explicit form in the frequency domain, the viscoelastic solution can be obtained by using the correspondence principle, that is, replacing the elastic moduli or the wave velocities by the corresponding complex viscoelastic moduli and velocities. The time-domain solution is generally obtained by an inverse Fourier transform and, therefore, is a semi-analytical solution. In very simple cases, such as the case of wave propagation in a semi-infinite rod represented by a Maxwell model, a closed-form time-domain solution can be obtained (Christensen, 1982, p. 190).

3.10.1 Viscoacoustic media

We start with the frequency-domain Green's function for acoustic (dilatational) media and apply the correspondence principle. To obtain the Green function $G(x, z, x_0, z_0, t)$ for a 2-D acoustic medium, we need to solve the inhomogeneous scalar wave equation

$$\Delta G - \frac{1}{c_a^2}\partial^2_{tt} G = -4\pi\delta(x - x_0)\delta(z - z_0)\delta(t), \tag{3.196}$$

where x and z are the receiver coordinates, x_0 and z_0 are the source coordinates, and c_a is the acoustic-wave velocity. The solution to equation (3.196) is given by

$$G(x, z, x_0, z_0, t) = 2H\left(t - \frac{r}{c_a}\right)\left(t^2 - \frac{r^2}{c_a^2}\right)^{-1/2}, \tag{3.197}$$

where

$$r = \sqrt{(x - x_0)^2 + (z - z_0)^2}, \tag{3.198}$$

and H is Heaviside's function (Morse and Feshbach, 1953, p. 1363; Bleistein, 1984, p. 65). Taking a Fourier transform with respect to time, equation (3.197) gives

$$G(x, z, x_0, z_0, \omega) = 2\int_{r/c_a}^{\infty}\left(t^2 - \frac{r^2}{c_a^2}\right)^{-1/2}\exp(-\mathrm{i}\omega t)dt. \tag{3.199}$$

By making a change of variable $\tau = c_a(t/r)$, equation (3.199) becomes

$$G(x, z, x_0, z_0, \omega) = 2\int_{1}^{\infty}(\tau^2 - 1)^{-1/2}\exp\left(-\frac{\mathrm{i}\omega}{c_a}\tau\right)d\tau. \tag{3.200}$$

This expression is the integral representation of the zero-order Hankel function of the second kind (Morse and Feshbach, 1953, p. 1362):

$$G(x, z, x_0, z_0, \omega) = -\mathrm{i}\pi H_0^{(2)}\left(\frac{\omega r}{c_a}\right). \tag{3.201}$$

Using the correspondence principle, we replace the acoustic-wave velocity c_a by the complex velocity $v_c(\omega)$, which is equivalent to replacing the acoustic bulk modulus ρc_a^2 by the complex modulus $M(\omega) = \rho v_c^2(\omega)$. Then, the viscoacoustic Green's function is

$$G(x, z, x_0, z_0, \omega) = -\mathrm{i}\pi H_0^{(2)} \left[\frac{\omega r}{v_c(\omega)} \right]. \tag{3.202}$$

We set

$$G(-\omega) = G^*(\omega). \tag{3.203}$$

This equation ensures that the inverse Fourier transform of the Green function is real.

For the dilatational field, for instance (see Section 2.7.4), the frequency-domain solution is given by

$$\epsilon(\omega) = G(\omega)F(\omega), \tag{3.204}$$

where $F(\omega)$ is the time Fourier transform of the source wavelet.

A wavelet representative of typical seismic pulses is given by equations (2.233) and (2.234). Because the Hankel function has a singularity at $\omega = 0$, we assume $G = 0$ for $\omega = 0$, an approximation that has no significant effect on the solution. (Note, moreover, that $F(0)$ is small). The time-domain solution $\epsilon(t)$ is obtained by a discrete inverse Fourier transform. We have tacitly assumed that ϵ and $\partial_t \epsilon$ are zero at time $t = 0$.

3.10.2 Constant-Q viscoacoustic media

Let us consider the Green function problem in anelastic viscoacoustic media, based on the constant-Q model (Section 2.5). Equation (2.220) can be solved in terms of the Green function, which is obtained from

$$\Delta G - \frac{(\mathrm{i}\omega)^\beta}{b} G = -4\pi\delta(x - x_0)\delta(z - z_0). \tag{3.205}$$

Let us define the quantity

$$\Omega = -\mathrm{i}(\mathrm{i}\omega)^{\beta/2}. \tag{3.206}$$

Expressing equation (3.205) in terms of this quantity gives the Helmholtz equation

$$\Delta G + \left(\frac{\Omega}{\sqrt{b}} \right)^2 G = -4\pi\delta(x - x_0)\delta(z - z_0). \tag{3.207}$$

The solution to this equation is the zero-order Hankel function of the second kind (Morse and Feshbach, 1953, p. 1362),

$$G(x, z, x_0, z_0, \omega) = -\mathrm{i}\pi H_0^{(2)} \left(\frac{\Omega r}{\sqrt{b}} \right), \tag{3.208}$$

where r is given in equation (3.198). An alternative approach is to use the correspondence principle and replace the elastic wave velocity c_a in equation (3.201) by the complex velocity (2.213). When $\beta = 2$, we obtain the classical solution for the Green function in an acoustic medium (equation (3.201)). We require the condition (3.203) that ensures a real Green's function. The frequency-domain solution is given by

$$w(\omega) = G(\omega)F(\omega), \tag{3.209}$$

where F is the Fourier transform of the source. As before, we assume $G = 0$ for $\omega = 0$ in order to avoid the singularity. The time-domain solution $w(t)$ is obtained by a discrete inverse Fourier transform.

We have seen in Section 2.5.2 that constant-Q propagation is governed by an evolution equation based on fractional derivates. Mainardi and Tomirotti (1997) obtained the fundamental solutions for the 1-D version of equation (2.220) in terms of entire functions of the Wright type. Let us consider this equation and define $\beta = 2\eta$. Mainardi and Tomirotti (1997) define the *signalling problem* as

$$\frac{\partial^{2\eta} w}{\partial t^{2\eta}} = b\partial_1^2 w, \quad w(x, 0^+) = 0, (x > 0); \quad w(0^+, t) = \delta(t), \quad w(+\infty, t) = 0, (t > 0). \tag{3.210}$$

The corresponding Green's function can be written as

$$G(x,t) = \frac{\eta x}{\sqrt{b} t^{1+\eta}} W_{-\eta, 1-\eta}(-\bar{x}), \qquad \bar{x} = \frac{x}{\sqrt{b} t^{\eta}}, \tag{3.211}$$

where

$$W_{q,r}(\bar{x}) = \sum_{k=0}^{\infty} \frac{\bar{x}^k}{k! \, \Gamma(qk + r)}, \qquad q > -1, \quad r > 0 \tag{3.212}$$

is the Wright function (Podlubny, 1999). The exponential and Bessel functions are particular cases of the Wright function (e.g., Podlubny, 1999). For instance, $W_{0,1}(\bar{x}) = \exp(\bar{x})$.

3.10.3 Viscoelastic media

The solution of the wave field generated by an impulsive point force in a 2-D elastic medium is given by Eason, Fulton and Sneddon (1956) (see also Pilant, 1979, p. 59). For a force acting in the positive z-direction, this solution can be expressed as

$$u_1(r,t) = \left(\frac{F_0}{2\pi\rho} \right) \frac{xz}{r^2} [G_1(r,t) + G_3(r,t)], \tag{3.213}$$

$$u_3(r,t) = \left(\frac{F_0}{2\pi\rho} \right) \frac{1}{r^2} [z^2 G_1(r,t) - x^2 G_3(r,t)], \tag{3.214}$$

where F_0 is a constant that gives the magnitude of the force, $r = \sqrt{x^2 + z^2}$,

$$G_1(r,t) = \frac{1}{c_P^2}(t^2 - \tau_P^2)^{-1/2} H(t - \tau_P) + \frac{1}{r^2}\sqrt{t^2 - \tau_P^2}\, H(t - \tau_P) - \frac{1}{r^2}\sqrt{t^2 - \tau_S^2}\, H(t - \tau_S) \tag{3.215}$$

and

$$G_3(r,t) = -\frac{1}{c_S^2}(t^2 - \tau_S^2)^{-1/2} H(t - \tau_S) + \frac{1}{r^2}\sqrt{t^2 - \tau_P^2}\, H(t - \tau_P) - \frac{1}{r^2}\sqrt{t^2 - \tau_S^2}\, H(t - \tau_S), \tag{3.216}$$

where

$$\tau_P = \frac{r}{c_P}, \qquad \tau_S = \frac{r}{c_S} \tag{3.217}$$

and c_P and c_S are the compressional and shear phase velocities. To apply the correspondence principle, we need the frequency-domain solution. Using the transform pairs of the zero- and first-order Hankel functions of the second kind,

$$\int_{-\infty}^{\infty} \frac{1}{\tau^2}\sqrt{t^2-\tau^2}H(t-\tau)\exp(-\mathrm{i}\omega t)dt = \frac{\mathrm{i}\pi}{2\omega\tau}H_1^{(2)}(\omega\tau), \tag{3.218}$$

$$\int_{-\infty}^{\infty} (t^2-\tau^2)^{-1/2}H(t-\tau)\exp(-\mathrm{i}\omega t)dt = -\frac{\mathrm{i}\pi}{2}H_0^{(2)}(\omega\tau), \tag{3.219}$$

we obtain

$$u_1(r,\omega,c_P,c_S) = \left(\frac{F_0}{2\pi\rho}\right)\frac{xz}{r^2}[G_1(r,\omega,c_P,c_S)+G_3(r,\omega,c_P,c_S)], \tag{3.220}$$

$$u_3(r,\omega,c_P,c_S) = \left(\frac{F_0}{2\pi\rho}\right)\frac{1}{r^2}[z^2G_1(r,\omega,c_P,c_S)-x^2G_3(r,\omega,c_P,c_S)], \tag{3.221}$$

where

$$G_1(r,\omega,c_P,c_S) = -\frac{\mathrm{i}\pi}{2}\left[\frac{1}{c_P^2}H_0^{(2)}\left(\frac{\omega r}{c_P}\right)+\frac{1}{\omega r c_S}H_1^{(2)}\left(\frac{\omega r}{c_S}\right)-\frac{1}{\omega r c_P}H_1^{(2)}\left(\frac{\omega r}{c_P}\right)\right], \tag{3.222}$$

$$G_3(r,\omega,c_P,c_S) = \frac{\mathrm{i}\pi}{2}\left[\frac{1}{c_S^2}H_0^{(2)}\left(\frac{\omega r}{c_S}\right)-\frac{1}{\omega r c_S}H_1^{(2)}\left(\frac{\omega r}{c_S}\right)+\frac{1}{\omega r c_P}H_1^{(2)}\left(\frac{\omega r}{c_P}\right)\right]. \tag{3.223}$$

Using the correspondence principle, we replace the elastic wave velocities in (3.220) and (3.221) by the viscoelastic wave velocities v_P and v_S defined in (3.18). The 2-D viscoelastic Green's function can then be expressed as

$$u_1(r,\omega) = \begin{cases} u_1(r,\omega,v_P,v_S), & \omega \geq 0, \\ u_1^*(r,-\omega,v_P,v_S), & \omega < 0, \end{cases} \tag{3.224}$$

and

$$u_3(r,\omega) = \begin{cases} u_3(r,\omega,v_P,v_S), & \omega \geq 0, \\ u_3^*(r,-\omega,v_P,v_S), & \omega < 0. \end{cases} \tag{3.225}$$

Multiplication with the source time function and a numerical inversion by the discrete Fourier transform yield the desired time-domain solution (G_1 and G_3 are assumed to be zero at $\omega = 0$).

3.11 The elastodynamic of a non-ideal interface

In seismology, exploration geophysics and several branches of mechanics (for example, metallurgical defects, adhesive joints, frictional contacts and composite materials), the problem of imperfect contact between two media is of particular interest. Seismological applications include wave propagation through dry and partially saturated cracks and fractures present in the Earth's crust, which may constitute possible earthquake sources. Similarly, in oil exploration, the problem finds applications in hydraulic fracturing, where a fluid is injected through a borehole to open a fracture in the direction of the least principal stress. Active and passive seismic waves are used to monitor the position and geometry of the fracture. In addition, in material science, a suitable model of an imperfect interface is necessary, since strength and fatigue resistance can be degraded by subtle differences between microstructures of the interface region and the bulk material.

Theories that consider imperfect bonding are mainly based on the displacement discontinuity model at the interface. Pyrak-Nolte, Myer and Cook (1990) propose a non-welded interface model based on the discontinuity of the displacement and the particle velocity across the interface. The stress components are proportional to the displacement discontinuity through the specific stiffnesses, and to the particle-velocity discontinuity through the specific viscosity. Displacement discontinuities conserve energy and yield frequency dependent reflection and transmission coefficients. On the other hand, particle-velocity discontinuities imply an energy loss at the interface and frequency-independent reflection and transmission coefficients. The specific viscosity accounts for the presence of a liquid under saturated conditions. The liquid introduces a viscous coupling between the two surfaces of the fracture (Schoenberg, 1980) and enhances energy transmission. However, at the same time, energy transmission is reduced by viscous losses.

3.11.1 The interface model

Consider a planar interface in an elastic and isotropic homogeneous medium; that is, the material on both sides of the interface is the same. The non-ideal characteristics of the interface are modeled through the boundary conditions between the two half-spaces. If the displacement and the stress field are continuous across the interface (ideal or welded contact), the reflection coefficient is zero and the interface cannot be detected. However, if the half-spaces are in non-ideal contact, reflected waves with appreciable amplitude can exist. The model is based on the discontinuity of the displacement and particle velocity fields across the interface.

Let us assume in this section the two-dimensional P-SV case in the (x, z)-plane, and refer to the upper and lower half-spaces with the labels I and II, respectively. Then, the boundary conditions for a wave impinging on the interface ($z = 0$) are

$$[v_1] \equiv (v_1)_{II} - (v_1)_I = \psi_1 * \partial_t \sigma_{13}, \tag{3.226}$$

$$[v_3] \equiv (v_3)_{II} - (v_3)_I = \psi_3 * \partial_t \sigma_{33}, \tag{3.227}$$

$$(\sigma_{13})_I = (\sigma_{13})_{II}, \tag{3.228}$$

$$(\sigma_{33})_I = (\sigma_{33})_{II}, \tag{3.229}$$

where v_1 and v_3 are the particle-velocity components, σ_{13} and σ_{33} are the stress components, and ψ_1 and ψ_3 are relaxation-like functions of the Maxwell type governing the tangential and normal coupling properties of the interface. The relaxation functions can be expressed as

$$\psi_i(t) = \frac{1}{\eta_i} \exp(-t/\tau_i) H(t), \quad \tau_i = \frac{\eta_i}{p_i}, \qquad i = 1, 3, \tag{3.230}$$

where $H(t)$ is Heaviside's function, $p_1(x)$ and $p_3(x)$ are specific stiffnesses, and $\eta_1(x)$ and $\eta_3(x)$ are specific viscosities. They have dimensions of stiffness and viscosity per unit length, respectively.

In the frequency domain, equations (3.226) and (3.227) can be compactly rewritten as

$$[v_i] = M_i \sigma_{i3}, \quad i = 1, 3, \tag{3.231}$$

where

$$M_i(\omega) = \mathcal{F}(\partial_t \psi_i) = \frac{\mathrm{i}\omega}{p_i + \mathrm{i}\omega\eta_i} \tag{3.232}$$

(see equation (2.147)) is a specific complex modulus having dimensions of admittance (reciprocal of impedance).

The characteristics of the medium are completed with the stress-strain relations. In isotropic media, stresses and particle velocities are related by the following equations:

$$\rho \partial_t \sigma_{11} = {I_P}^2 \partial_1 v_1 + ({I_P}^2 - 2I_S^2) \partial_3 v_3, \tag{3.233}$$

$$\rho \partial_t \sigma_{33} = ({I_P}^2 - 2{I_S}^2) \partial_1 v_1 + {I_P}^2 \partial_3 v_3, \tag{3.234}$$

$$\rho \partial_t \sigma_{13} = {I_S}^2 \left(\partial_1 v_3 + \partial_3 v_1 \right), \tag{3.235}$$

where $I_P = \rho c_P$ and $I_S = \rho c_S$ are the compressional and shear impedances, with c_P and c_S denoting the elastic wave velocities, respectively.

Boundary conditions in differential form

The boundary equations (3.226) and (3.227) could be implemented in a numerical solution algorithm. However, the evaluation of the convolution integrals is prohibitive when solving the differential equations with grid methods. In order to circumvent the convolutions, we recast the boundary conditions in differential form. From equations (3.226) and (3.227), and using convolution properties, we have

$$[v_i] = \partial_t \psi_i * \sigma_{i3}. \tag{3.236}$$

Using equation (3.230) and after some calculations, we note that

$$[v_i] = \psi_i(0)\sigma_{i3} - \frac{1}{\tau_i} \psi_i * \sigma_{i3}. \tag{3.237}$$

Since $[v_i] = \partial_t [u_i]$, where u_i is the displacement field, we can infer from equation (3.236) that

$$[u_i] = \psi_i * \sigma_{i3}. \tag{3.238}$$

Then, equation (3.237) becomes

$$\partial_t [u_i] = \frac{1}{\eta_i} (\sigma_{i3} - p_i [u_i]). \tag{3.239}$$

Alternatively, this equation can be written as

$$p_i [u_i] + \eta_i [v_i] = \sigma_{i3}. \tag{3.240}$$

Note that $p_i = 0$ gives the displacement discontinuity model, and $\eta_i = 0$ gives the particle-velocity discontinuity model. On the other hand, if $\eta_i \to \infty$ (see equation (3.239)), the model gives the ideal (welded) interface.

3.11.2 Reflection and transmission coefficients of SH waves

The simplicity of the SH case permits a detailed treatment of the reflection and transmission coefficients, and provides some insight into the nature of energy loss in the more cumbersome P-SV problem. We assume an interface separating two dissimilar materials of shear impedances I_S^I and I_S^{II}. The theory, corresponding to a specific stiffness p_2 and a specific viscosity η_2, satisfies the following boundary conditions:

$$(v_2)_{II} - (v_2)_I = \psi_2 * \partial_t \sigma_{23}, \tag{3.241}$$

$$(\sigma_{23})_I = (\sigma_{23})_{II}, \tag{3.242}$$

where

$$\rho \sigma_{23} = I_S^2 \partial_3 u_2, \tag{3.243}$$

and u_2 is the displacement field. The relaxation function ψ_2 has the same form (3.230), where $i = 2$.

In half-space I, the displacement field is

$$u_2)_I = \exp[\mathrm{i}\kappa^I (x \sin\theta + z\cos\theta)] + R_{\mathrm{SS}} \exp[\mathrm{i}\kappa^I (x\sin\theta - z\cos\theta)], \tag{3.244}$$

where κ^I is the real wavenumber and R_{SS} is the reflection coefficient. In half-space II, the displacement field is

$$u_2)_{II} = T_{\mathrm{SS}} \exp[\mathrm{i}\kappa^{II} (x\sin\delta + z\cos\delta)], \tag{3.245}$$

where T_{SS} is the transmission coefficient and

$$\delta = \arcsin\left(\frac{\kappa^I}{\kappa^{II}}\right)\sin\theta,$$

according to Snell's law. For clarity, the factor $\exp(-\mathrm{i}\omega t)$ has been omitted in equations (3.244) and (3.245).

Considering that $v_2 = -\mathrm{i}\omega u_2$, the reflection and transmission coefficients are obtained by substituting the displacements into the boundary conditions. This gives

$$R_{\mathrm{SS}} = \frac{Y_I - Y_{II} + Z}{Y_I + Y_{II} + Z}, \qquad T_{\mathrm{SS}} = \frac{2Y_I}{Y_I + Y_{II} + Z}, \tag{3.246}$$

where

$$Y_I = I_S^I \cos\theta \quad \text{and} \quad Y_{II} = I_S^{II}\cos\delta, \tag{3.247}$$

$$Z(\omega) = Y_I Y_{II} M_2(-\omega), \tag{3.248}$$

and the relation $\kappa^{I(II)} I_S^{I(II)} = \rho\omega$ has been used.

Since

$$M_2(\omega) = \frac{\mathrm{i}\omega}{p_2 + \mathrm{i}\omega\eta_2}, \tag{3.249}$$

the reflection and transmission coefficients are frequency independent for $p_2 = 0$ and, moreover, there are no phase changes. In this case, when $\eta_2 \to 0$, $R_{\mathrm{SS}} \to 1$ and $T_{\mathrm{SS}} \to 0$, and the free-surface condition is obtained; when $\eta_2 \to \infty$, $R_{\mathrm{SS}} \to 0$ and $T_{\mathrm{SS}} \to 1$, the ideal (welded) interface is obtained

Energy loss

In a completely welded interface, the normal component of the time-averaged energy flux is continuous across the plane separating the two media. This is a consequence of the boundary conditions that impose continuity of normal stress and particle velocity. The normal component of the time-averaged energy flux is proportional to the real part of $\sigma_{23}v_2^*$. Since the media are elastic, the interference terms between different waves (see Section 6.1.7) vanish and only the fluxes corresponding to each single beam need be considered. After normalizing with respect to the incident wave, the energy fluxes of the reflected and transmitted waves are

$$\text{reflected wave} \rightarrow |R_{\rm SS}|^2, \tag{3.250}$$

$$\text{transmitted wave} \rightarrow \frac{Y_{II}}{Y_I}|T_{\rm SS}|^2. \tag{3.251}$$

The energy loss at the interface is obtained by subtracting the energies of the reflected and transmitted waves from the energy of the incident wave. The normalized dissipated energy is

$$\mathcal{D} = 1 - |R_{\rm SS}|^2 - \frac{Y_{II}}{Y_I}|T_{\rm SS}|^2. \tag{3.252}$$

Substituting the reflection and transmission coefficients, we note that the energy loss becomes

$$\mathcal{D} = \frac{4Y_{II}Z_R}{(Y_I + Y_{II} + Z_R)^2 + Z_I^2}, \tag{3.253}$$

where Z_R and Z_I are the real and imaginary parts of Z, given by

$$Z_R = \frac{\omega^2\eta_2 Y_I Y_{II}}{p_2^2 + \omega^2\eta_2^2}, \quad \text{and} \quad Z_I = \frac{\omega p_2 Y_I Y_{II}}{p_2^2 + \omega^2\eta_2^2}. \tag{3.254}$$

If $p_2 = 0$, then $Z_I = 0$, $Z_R = Y_I Y_{II}/\eta_2$, and the energy loss is frequency independent. When $\eta_2 \rightarrow 0$ (complete decoupling) and $\eta_2 \rightarrow \infty$ (welded contact), there is no energy dissipation. If $p_2 = 0$, the maximum loss is obtained for

$$\eta_2 = \frac{Y_I Y_{II}}{Y_I + Y_{II}}. \tag{3.255}$$

At normal incidence and in equal lower and upper media, this gives $\eta_2 = I_S/2$, and a (normalized) energy loss $\mathcal{D} = 0.5$, i.e., half of the energy of the normally incident wave is dissipated at the interface.

3.11.3 Reflection and transmission coefficients of P-SV waves

Consider an interface separating two half-spaces with equal material properties, where the boundary conditions are given by equations (3.226)-(3.229). Application of Snell's law indicates that the angle of the transmitted wave is equal to the angle of the incident wave, and that

$$\kappa_P \sin\theta = \kappa_S \sin\alpha,$$

where κ_P and κ_S are the real compressional and shear wavenumbers, and θ and α are the respective associated angles. The boundary conditions do not influence the emergence angles of the transmitted and reflected waves.

In terms of the dilatational and shear potentials ϕ and ψ, the displacements are given by

$$u_1 = \partial_1\phi - \partial_3\psi, \quad \text{and} \quad u_3 = \partial_3\phi + \partial_1\psi, \tag{3.256}$$

(Pilant, 1979, p. 45) and the stress components by

$$\sigma_{13} = \frac{I_S^2}{\rho}\left(2\partial_1\partial_3\phi + \partial_1\partial_1\psi - \partial_3\partial_3\psi\right), \tag{3.257}$$

and

$$\sigma_{33} = \frac{I_P^2}{\rho}\left(\partial_1\partial_1\phi + \partial_3\partial_3\phi\right) - \frac{2I_S^2}{\rho}\left(\partial_1\partial_1\phi - \partial_1\partial_3\psi\right). \tag{3.258}$$

Consider a compressional wave incident from half-space I. Then, the potentials of the incident and reflected waves are

$$\phi^I = \exp[\mathrm{i}\kappa_P(x\sin\theta + z\cos\theta)], \tag{3.259}$$

$$\phi^R = R_{\mathrm{PP}}\exp[\mathrm{i}\kappa_P(x\sin\theta - z\cos\theta)], \tag{3.260}$$

and

$$\psi^R = R_{\mathrm{PS}}\exp[\mathrm{i}\kappa_S(x\sin\alpha - z\cos\alpha)]. \tag{3.261}$$

In half-space II, the potentials of the transmitted wave are

$$\phi^T = T_{\mathrm{PP}}\exp[\mathrm{i}\kappa_P(x\sin\theta + z\cos\theta)], \tag{3.262}$$

and

$$\psi^T = T_{\mathrm{PS}}\exp[\mathrm{i}\kappa_S(x\sin\alpha + z\cos\alpha)]. \tag{3.263}$$

Considering that $v_1 = -\mathrm{i}\omega u_1$ and $v_3 = -\mathrm{i}\omega u_3$, the solution for an incident P wave is

$$\begin{pmatrix} \sin\alpha\,(1 + 2\gamma_1 I_{\mathrm{SP}}\cos\theta) & \cos\alpha + \gamma_1\cos 2\alpha & -\sin\alpha & \cos\alpha \\ -\gamma_3\cos 2\alpha - \cos\theta & \sin\theta + \gamma_3\sin 2\alpha & -\cos\theta & -\sin\theta \\ 2I_{\mathrm{SP}}\sin\alpha\cos\theta & \cos 2\alpha & 2I_{\mathrm{SP}}\sin\alpha\cos\theta & -\cos 2\alpha \\ -\cos 2\alpha & \sin 2\alpha & \cos 2\alpha & \sin 2\alpha \end{pmatrix}$$

$$\cdot \begin{pmatrix} R_{\mathrm{PP}} \\ R_{\mathrm{PS}} \\ T_{\mathrm{PP}} \\ T_{\mathrm{PS}} \end{pmatrix} = \begin{pmatrix} -\sin\alpha\,(1 - 2\gamma_1 I_{\mathrm{SP}}\cos\theta) \\ \gamma_3\cos 2\alpha - \cos\theta \\ 2I_{\mathrm{SP}}\sin\alpha\cos\theta \\ \cos 2\alpha \end{pmatrix}, \tag{3.264}$$

where $I_{\mathrm{SP}} = I_S/I_P$,

$$\gamma_1 = I_S M_1(-\omega) = \frac{\mathrm{i}\omega I_S}{\mathrm{i}\omega\eta_1 - p_1} \quad \text{and} \quad \gamma_3 = I_P M_3(-\omega) = \frac{\mathrm{i}\omega I_P}{\mathrm{i}\omega\eta_3 - p_3}, \tag{3.265}$$

and the following relations have been used:

$$I_S\kappa_S = \rho\omega, \qquad I_P\kappa_P = \rho\omega, \tag{3.266}$$

and

$$\rho\mu = I_S^2, \qquad \rho\lambda = I_P^2 - 2I_S^2. \tag{3.267}$$

Equations (3.264), which yield the potential amplitude coefficients, were obtained by Carcione (1996a) to investigate the scattering of cracks and fractures. Chiasri and Krebes (2000) obtain similar expressions for the displacement amplitude coefficients. The multiplying conversion factor from one type of coefficient to the other is 1 for PP coefficients and I_S/I_P for PS coefficients (Aki and Richards, 1980, p. 139).

The reflection and transmission coefficients for a P wave at normal incidence are

$$R_{\rm PP} = -\left(1 + \frac{2}{\gamma_3}\right)^{-1} \tag{3.268}$$

and

$$T_{\rm PP} = \left(1 + \frac{\gamma_3}{2}\right)^{-1}, \tag{3.269}$$

respectively. If $\eta_3 = 0$, the coefficients given in Pyrak-Nolte, Myer and Cook (1990) are obtained. If, moreover, $p_3 \rightarrow 0$, $R_{\rm PP} \rightarrow -1$ and $T_{\rm PP} \rightarrow 0$, the free-surface condition is obtained; when $\eta_3 \rightarrow \infty$, $R_{\rm PP} \rightarrow 0$ and $T_{\rm PP} \rightarrow 1$, we get the solution for a welded contact. On the other hand, it can be seen that $\eta_3 = 0$ and $p_3 = \omega I_P/2$ gives $|R_{\rm PP}|^2 = 1/2$. The characteristic frequency $\omega_P \equiv 2p_3/I_P$ defines the transition from the apparently perfect interface to the apparently delaminated one.

The reflection and transmission coefficients corresponding to an incident SV wave can be obtained in the same way as for the incident P wave. In particular, the coefficients of the normally incident wave, $R_{\rm SS}$ and $T_{\rm SS}$, have the same form as in equations (3.268) and (3.269), but γ_1 is substituted for γ_3.

Energy loss

Following the procedure used to obtain the energy flow in the SH case, we get the following normalized energies for an incident P wave:

$$\begin{array}{lcc} \text{reflected P wave} & \rightarrow & |R_{\rm PP}|^2, \\ \text{reflected S wave} & \rightarrow & \dfrac{\tan\theta}{\tan\alpha}|R_{\rm PS}|^2, \\ \text{transmitted P wave} & \rightarrow & |T_{\rm PP}|^2, \\ \text{transmitted S wave} & \rightarrow & \dfrac{\tan\theta}{\tan\alpha}|T_{\rm PS}|^2. \end{array} \tag{3.270}$$

Hence, the normalized energy loss is

$$\mathcal{D} = 1 - |R_{\rm PP}|^2 - |T_{\rm PP}|^2 - \frac{\tan\theta}{\tan\alpha}(|R_{\rm PS}|^2 + |T_{\rm PS}|^2). \tag{3.271}$$

It can be easily shown that the amount of dissipated energy at normal incidence is

$$\mathcal{D} = \frac{4\gamma_{3R}}{(2 + \gamma_{3R})^2 + \gamma_{3I}^2}, \tag{3.272}$$

where the subindices R and I denote real and imaginary parts, respectively. If $p_3 = 0$, the maximum loss is obtained for $\eta_3 = I_P/2$. Similarly, if $p_1 = 0$, the maximum loss for an incident SV wave occurs when $\eta_1 = I_S/2$.

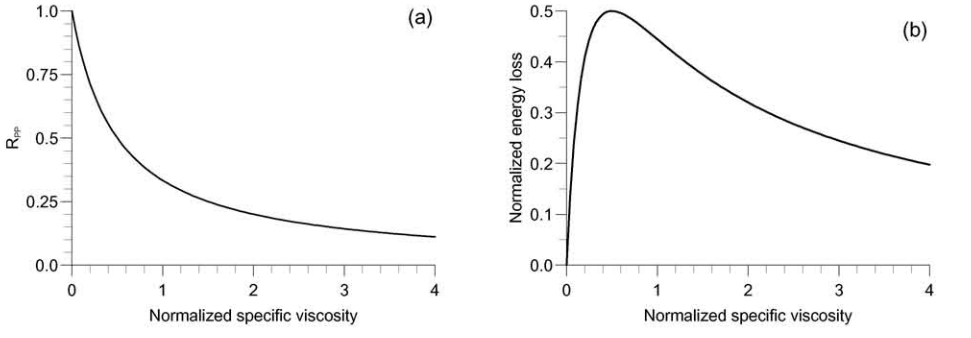

Figure 3.7: Non-ideal interface in a homogeneous medium. Normal incidence reflection coefficient $R_{\rm PP}$ (a) and normalized energy loss $\mathcal{D}$ (b) at $\theta = 0$ versus normalized specific viscosity η_3/I_P. Only the particle-velocity discontinuity ($p_3 = 0$) has been considered. As $\eta_3 \rightarrow 0$, complete decoupling (free-surface condition) is obtained. As $\eta_3 \rightarrow \infty$, the contact is welded. The maximum dissipation occurs for $\eta_3 = I_P/2$.

Examples

The following example considers a crack in a homogeneous medium bounded by a free surface. The medium is a Poisson solid with compressional and shear velocities $c_P = I_P/\rho = 2000$ m/s and $c_S = I_S/\rho = 1155$ m/s, respectively, and density $\rho = 2$ g/cm^3. Figure 3.7 represents the normal incidence reflection coefficient $R_{\rm PP}$ (a) and the normalized energy loss (b) versus the normalized specific viscosity η_3/I_P, with $p_3 = 0$. As can be seen, the limit $\eta_3 \rightarrow 0$ gives the complete decoupled case, and the limit $\eta_3 \rightarrow \infty$ gives the welded interface, since $R_{\rm PP} \rightarrow 0$. The maximum dissipation occurs for $\eta_3 = I_P/2$. Similar plots and conclusions are obtained for an incident SV wave, for which the maximum loss occurs when $\eta_1 = I_S/2$. It can be shown that, for any incidence angle and values of the specific stiffnesses, there is no energy loss when $\eta_3 \rightarrow 0$ and $\eta_3 \rightarrow \infty$.

In the second example, we consider two different cases. The first case has the parameters $\eta_1 = I_S/2$ and $\eta_3 = I_P/2$ and zero specific stiffnesses. Figure 3.8 represents the reflection and transmission coefficients for an incident compressional wave (a) and the energy loss (b) versus the incidence angle (equation (3.264)). As can be seen, the dissipated energy is nearly 50 % up to 80°.

The second case has the following parameters: $p_1 = \pi f_0 I_S$, $p_3 = \pi f_0 I_P$, $\eta_1 = I_S/100$ and $\eta_3 = I_P/100$, where $f_0 = 11$ Hz. The model is practically based on the discontinuity of the displacement field. Figure 3.9 represents the reflection and transmission coefficients for an incident compressional wave versus the incidence angle. In this case, the energy loss is nearly 2 % of the energy of the incident wave.

Figure 3.10 shows a snapshot of the vertical particle velocity v_3 when the crack surface satisfies stress-free boundary conditions. Energy is conserved and there is no transmission through the crack. Two Rayleigh waves, traveling along the crack plane, can be appreciated.

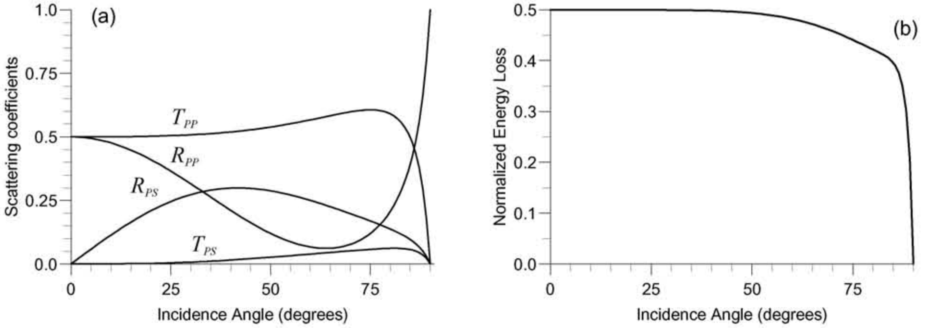

Figure 3.8: Non-ideal interface in a homogeneous medium. Reflection and transmission coefficients (a) and normalized energy loss $\mathcal{D}$ (b) versus incidence angle θ for a fracture defined by the following specific stiffnesses and viscosities: $p_1 = p_3 = 0$, $\eta_1 = I_S/2$ and $\eta_3 = I_P/2$.

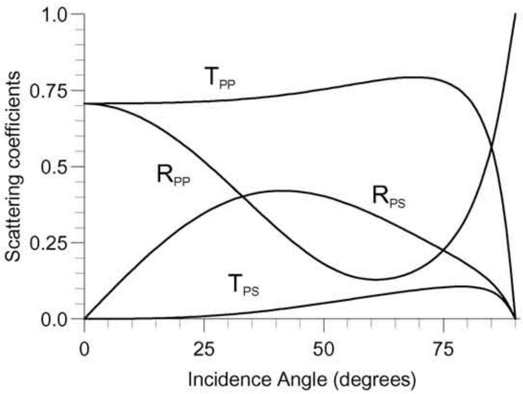

Figure 3.9: Reflection and transmission coefficients versus incidence angle θ for a non-ideal interface defined by the following specific stiffnesses and viscosities: $p_1 = \pi f_0 I_S$ and $p_3 = \pi f_0 I_P$, and $\eta_1 = I_S/100$ and $\eta_3 = I_P/100$, where $f_0 = 11$ Hz.

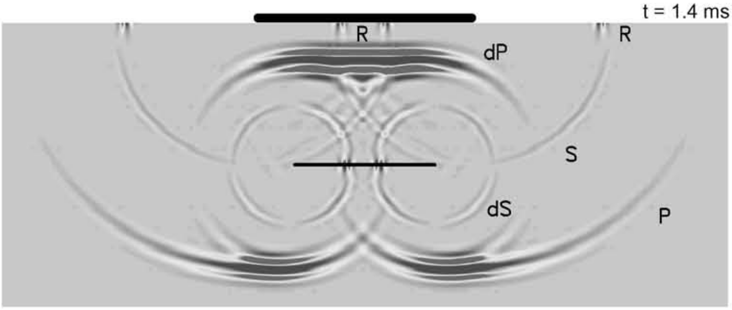

Figure 3.10: Vertical surface load radiation and crack scattering. The snapshot shows the v_3-component at 1.4 ms. "R" denotes the Rayleigh wave, "P" the compressional wave, "S" the shear wave, and "dP" and "dS" the compressional and shear waves diffracted by the crack tips, respectively. The size of the model is 75 $\times$ 30 cm, and the source central frequency is 110 kHz. The crack is at 14.6 cm from the surface and is 14.4 cm in length. The specific stiffnesses and viscosities of the crack are zero, implying a complete decoupling of the crack surfaces (Carcione, 1996a).